AGE AND THERMAL DIFFUSION LENGTH OF PLUTONIUM-BERYLLIUM NEUTRONS IN POISONED WATER

by

Marshall Thomas Slayton

United States
Naval Postgraduate School

THESIS

AGE AND THERMAL DIFFUSION LENGTH
OF PLUTONIUM-BERYLLIUM NEUTRONS
IN POISONED WATER

by

Marshall Thomas Slayton

June 1970

Age and Thermal Diffusion Length of Plutonium-Beryllium Neutrons in Poisoned Water

by

Marshall Thomas Slayton
Commander, United States Navy
B.S., United States Naval Academy, 1955

Submitted in partial fulfillment of the
requirements for the degree of

MASTER OF SCIENCE IN MECHANICAL ENGINEERING

from the

NAVAL POSTGRADUATE SCHOOL
June 1970

ABSTRACT

Measurements of Pu-Be neutron age to indium resonance and thermal migration area were made in pure water at 24°C and in mixtures containing 1.16, 8.96, 27.81, 46.65, 70.09, and 80.09 grams/liter of boric acid at 40°C. Thermal diffusion lengths were calculated from these measurements and the dependence on poison concentration observed. It was concluded, both from failure of the age measurement and the irresolute thermal flux behavior at the heaviest poison concentration, that the "maximum absorption" limit was exceeded in this experiment. The absorption cross-section of the supporting medium corresponding to the 80.09 g/l concentration was 0.6120 cm^{-1}. The present results, together with previous experimental data, provide an estimate of diffusion length at the absorption limit of 0.5 cm, slightly less than that corresponding to the theoretical Corngold limit (0.6 cm).

TABLE OF CONTENTS

ACKNOWLEDGMENT

The author is pleased to acknowledge his indebtedness to Professor D. H. Nguyen for his expert and conscientious guidance throughout the course of the investigation. The many inspiring discussions by him, particularly those concerned with the exploration of procedures suitable for making measurements with a Pu-Be source, were essential to the attainment of research objectives. Special thanks are due to Professor P. J. Marto for his thorough review of an earlier version of this report and the recommendations he gave for its improvement. The method of chemical analysis used in determining boron concentrations was obtained from Professor C. F. Rowell. His genuine eagerness to help in this area is gratefully acknowledged. To my wife Lucy go my thanks and admiration, both for her patience and her invaluable assistance in the typing of the many rough stages of the report.

I. INTRODUCTION

It has been shown analytically by Corngold [1] that if the absorption concentration of a supporting medium is increased beyond a certain value (assuming 1/v absorption in an infinite medium), no thermal neutron diffusion length exists. The practical implication of this is that under such extreme circumstances the spatial distribution of thermal neutrons cannot be resolved. Table 1 lists theoretical values of the minimum diffusion length which corresponds to the "maximum absorption" limit for the more common moderators [2].

TABLE 1

Moderator	Minimum Diffusion Length (cm)
C	23
Be	18
H_2O	0.6
D_2O	2.8

The dependence of thermal neutron diffusion length upon the absorption concentration in water has been the subject of several experiments [3, 4, 5]. In all of these experiments the limiting value of diffusion length is assumed, but not proved.

The most extensive measurements of diffusion length in water poisoned with a 1/v absorber have been those by Goddard and Johnson [3]. Their work included measurements in water containing dissolved boron which was ideally suited for the purpose. Boron is a strong 1/v absorber, i.e.,its cross-section varies inversely with neutron velocity, or as the square root of neutron kinetic energy. Therefore, the homogenious mixing of small amounts with pure water has negligible effect on the average scattering cross-section but drastically increases the absorption cross-section.

Goddard and Johnson experimented with a wide range of boron concentrations at temperatures of 22.3° and 65°C. Their most heavily absorbing solution contained 69.3 g/l of boric acid (H_3BO_3) and gave a diffusion length measurement of 0.6581 cm (within the Corngold limit). Similar measurements using dissolved cadmium at concentrations of 55.5 and 82.2 g/l resulted in measurements of 0.5983 and 0.4925 cm respectively, both of which lay outside the Corngold limit. They did not report any difficulties in obtaining these latter diffusion lengths.

This research project aimed at experimentally determining the "maximum absorption" limit by increasing the boron concentration in pure water beyond that attained by Goddard and Johnson until the diffusion length measurement failed.

This experiment was conducted using a plutonium-beryllium source which emitted 5.4×10^6 fast neutrons per second.

It will be explained in the following sections why this fast neutron source dictated an unconventional and indirect method of determining diffusion length. In the process, information concerning the dependence of neutron migration area and age on the poison concentration is obtained for the first time.

II. THEORY

A. TWO-GROUP DIFFUSION THEORY

The thermal neutron flux, in most cases, arises from a source of neutrons having energies many orders of magnitude larger than the energy of neutrons in thermal equilibrium with the medium (about .025 eV at 25°C) [6]. The Pu-Be (α,n) source used in this work yields neutrons with an average kinetic energy of about 4.2 MeV and the neutron spectrum ranges from roughly zero to about 10.6 MeV. The calculated spectrum is shown in Figure 1. [7]

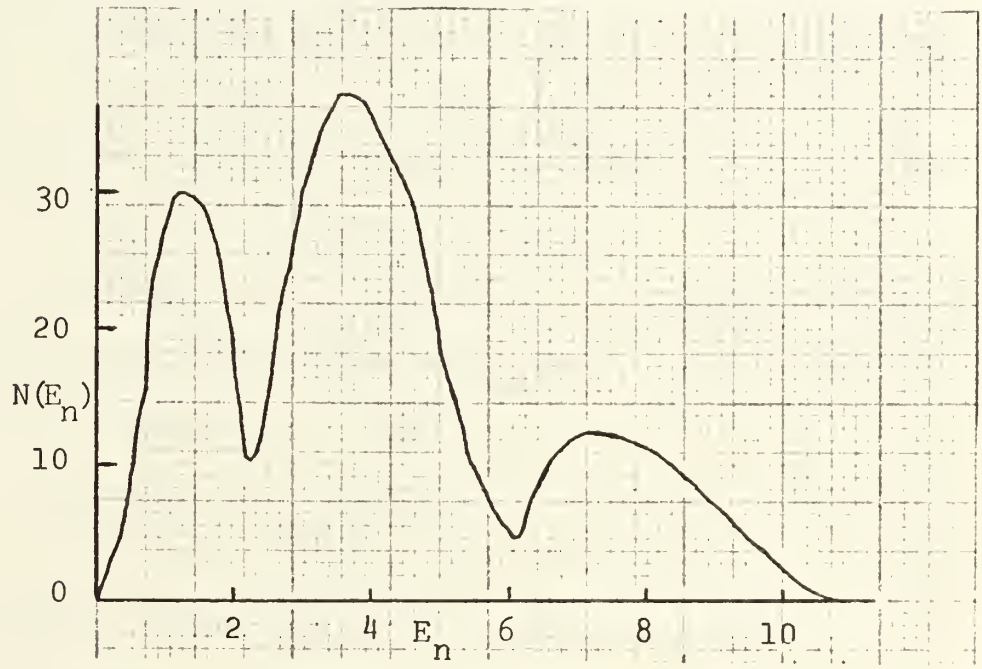

Figure 1. Calculated Neutron Spectrum for a Pu-Be Source.

The analytical model which describes the neutron population as two separate groups, one fast and one thermal, gives solutions which approximate the behavior of neutrons in real

assemblies and for many practical calculations, is sufficiently accurate [8]. In the two-group treatment, neutrons of thermal energy constitute one group while all those of higher energy belong to the fast group. Neutrons are considered removed from the fast group by scattering collisions which reduce their energy to the thermal region. Since absorption cross-sections of moderators for high energy neutrons are very small, any loss of the fast neutrons by absorption is neglected.

The disappearance of neutrons from the fast group is described in terms of a "slowing down" cross section, Σ_F [6]. By denoting the fast neutron flux by ϕ_F (neutrons/cm^2-sec), Σ_F is defined such that $\Sigma_F\phi_F(r)$ gives the number of neutrons per cm^3/sec. which slow down out of the fast group at the point r cm from the source.

If an isotropic point source at r = 0 emits S fast neutrons/sec in an infinite moderator, the fast flux at $r \neq 0$ can be described by [7]

$$D_F\nabla^2\phi_F(r) - \Sigma_F\phi_F(r) = 0 \qquad (1)$$

where $\nabla^2\phi(r)$ is the Laplacian of the flux and D_F is the diffusion coefficient for the fast neutrons. The source at r = 0 is taken into account by means of a source condition which will be stated later in this section.

The quantity D_F can be derived by considering Fick's Law of Diffusion which states that the neutron current density is proportional to the negative gradient of the

flux. The proportionality constant has dimensions in length and is called the diffusion coefficient, denoted by D in the more general treatment of neutron diffusion. Accordingly, the fast neutron current density can be represented by [6].

$$\text{Fast Neutron Current Density} = -D_F \nabla \phi_F(r) = -\int_{E_{th}}^{E_0} D(E) \nabla \phi(r,E)\, dE$$

where the integral is evaluated over the energy region of the fast froup, i.e., from thermal, E_{th}, to source energy, E_0. The fast flux is defined by the integral

$$\phi_F(r) = \int_{E_{th}}^{E_0} \phi(r,E)\, dE$$

and therefore

$$D_F = \frac{\int_{E_{th}}^{E_0} D(E) \nabla \phi(r,E) dE}{\int_{E_{th}}^{E_0} \nabla \phi(r,E)\, dE}$$

In two-group theory it is assumed that the variation in the neutron flux spectrum from point to point in the medium can be neglected, that is the flux is completely separable in space and energy. Thus,

$$D_F = \frac{\int_{E_{th}}^{E_0} D(E)\phi(E)dE}{\int_{E_{th}}^{E_0} \phi(E)\, dE} \qquad (2)$$

where $\phi(E)$ is the energy dependent flux.

Returning to Equation (1), and using the boundary condition that $\phi_F(r)$ must remain finite as $r \to \infty$, the general solution can be obtained:

$$\phi_F(r) = C \frac{e^{-r/\sqrt{\tau_T}}}{r} \qquad (3)$$

where the parameter τ_T is known as the neutron age to thermal energies, defined here as [9]

$$\tau_T = \frac{D_F}{\Sigma_F} \qquad (4)$$

The constant C is found from the source condition which is obtained by drawing a small sphere around the source and computing the number of neutrons that pass through its surface per second. Considering the magnitude of the current density in fast neutrons per cm^2/sec, $J_F(r)$, and a sphere of radius r, this number is $4\pi r^2 J_F(r)$. Then, in the limit, as $r \to 0$, the source condition is

$$\lim_{r \to 0} 4\pi r^2 J_F(r) = S \qquad (5)$$

Thus

$$J_F(r) = -D_F \frac{d\phi_F(r)}{dr} = \frac{D_F C e^{-r/\sqrt{\tau_T}}}{r^2} \left[\frac{r}{\sqrt{\tau_T}} + 1\right]$$

and

$$C = \frac{S}{4\pi D_F}$$

Finally, the fast flux is given by

$$\phi_F(r) = \frac{S e^{-r/\sqrt{\tau_T}}}{4\pi r \tau_T \Sigma_F} \qquad (6)$$

Considering now the thermal neutron group, the time-independent diffusion equation which describes the thermal flux can be written

$$\bar{D}\nabla^2 \phi_T(r) - \bar{\Sigma}_a \phi_T(r) + q_T(r) = 0 \qquad (7)$$

where $\phi_T(r)$ is the thermal flux, $\bar{D}$ is the average value of the diffusion coefficient in the thermal region, $\bar{\Sigma}_a$ is the average macroscopic thermal absorption cross section and $q_T(r)$ is the thermal slowing down density. The quantity $q_T(r)$ is equivalent to the production rate of thermal neutrons per unit volume and, for the case of a point source of fast neutrons in an infinite moderator, is equal to $\Sigma_F\phi_F(r)$, the number of neutrons slowing down out of the fast group.

Equation(7) can be rewritten as

$$\nabla^2 \phi_T(r) - \frac{\phi_T(r)}{L_T^2} + \frac{\Sigma_F \phi_F(r)}{\bar{D}} = 0 \qquad (8)$$

where $\phi_F(r)$ is given by Equation (2) and $L_T = \left(\frac{\bar{D}}{\bar{\Sigma}_a}\right)^{\frac{1}{2}}$ is the thermal neutron diffusion length. By requiring the neutron flux to remain finite, the homogeneous solution becomes

$$\phi_T(r)_H = \frac{K_1 \, e^{-r/L_T}}{r} \, . \tag{9}$$

Since the source term is proportional to the fast flux, a particular solution is assumed of the form

$$\phi_T(r)_P = \frac{K_2 \, e^{-r/\sqrt{\tau_T}}}{r} \, , \tag{10}$$

By substituting this expression into Equation (8), the constant K_2 is found to be

$$K_2 = \frac{-S \, L_T^{\,2}}{4\pi \, \bar{D} \, (L_T^2 - \tau_T)} \, . \tag{11}$$

The general solution to Equation (8) can now be written

$$\phi_T(r) = \frac{K_1 \, e^{-r/L_T}}{r} - \frac{S \, L_T^{\,2} \, e^{-r/\sqrt{\tau_T}}}{4\pi r \, \bar{D} \, (L_T^{\,2} - \tau_T)} \tag{12}$$

where the constant K_1 can be determined by a source condition as in the fast flux case. However, since the source only produces fast neutrons, the required source condition for the thermal flux is

$$\lim_{r \to 0} 4\pi r^2 \, J_T(r) = 0 \tag{13}$$

where $J_T(r)$ is the magnitude of the thermal neutron current density. Thus,

$$J_T(r) = -\overline{D} \frac{d\phi_T(r)}{dr}$$

and the constant K_1 becomes

$$K_1 = \frac{S L_T^2}{4\pi \overline{D} (L_T^2 - \tau_T)} \tag{14}$$

Finally, the thermal flux is given by

$$\phi_T(r) = \frac{S}{4\pi r \overline{\Sigma}_a L_T^2 (1-\tau_T)} \left(e^{-r/L_T} - e^{-r/\sqrt{\tau_T}}\right) \tag{15}$$

Equation (15) describes the thermal neutron flux in neutrons per cm^2/sec in an infinite moderator using two-group theory.

It follows from the development of Equation (15) that it is also possible to describe the slowing down of the fast neutrons and their subsequent diffusion as thermal neutrons as two distinct processes. The neutron age, τ_T, is related to the distance traveled from the point where a fast neutron first appears to the point where it slows down to thermal energies. Similarly, the square of the thermal neutron diffusion length, L_T^2, corresponds to the distance traveled from the point where a neutron becomes thermal to the point where it is finally absorbed. A quantity M_T^2, known as the thermal migration area, takes

into account the total neutron travel during moderation and diffusion. Accordingly,

$$M_T^2 = L_T^2 + \tau_T \qquad (16)$$

where M_T (migration length), $\sqrt{\tau_T}$ (slowing down length) and L_T all have dimensions in length.

B. ONE-GROUP DIFFUSION APPROXIMATION

Although the two-group theory gives more accurate flux solutions, the one-group approximation readily accommodates the "first scattering source" theory which is useful for our analysis. In one-group diffusion theory all neutrons are lumped together into one-group, namely thermal. This approximation, while limiting the description of the neutron population to spatial dependence, allows attention to be focused on the diffusion process.

In the two-group model of the previous section, neutrons entered the thermal group as a result of slowing down out of the fast group, and the thermal slowing down density, $q_T(r)$, appeared as the source term in the thermal diffusion equation. In the one-group treatment, however, when the actual neutron source yields fast neutrons, the source term used for the diffusion equation must be altered to account for the behavior of the fast neutrons prior to reaching thermal energies. In the particular case of a point source emitting S fast neutrons/sec in an infinite media, the slowing down density at r is given by the relation [10]

$$q(r,\tau) = \frac{Se^{-r^2/4\tau}}{(4\pi\tau)^{3/2}} \qquad (17)$$

where τ is the neutron age. A small τ means that the neutrons have suffered little slowing down and so they have not diffused far from the source. Larger values of τ correspond to neutrons which have been slowing down longer and therefore have had an opportunity to diffuse further from the source. When the neutron age to thermal energies, τ_T, is substituted into Equation (17), the resulting expression gives the dispersion of thermal neutrons and can then be used as the source term for the diffusion equation.

Equation (17) is based on the Fermi age model which assumes that the slowing down process is a continuous one [9]. In hydrogeneous media, however, the slowing down process is not continuous due to the fact that a neutron may lose all of its energy following a collision with hydrogen. In addition, the hydrogen scattering cross section decreases rapidly with energy above about 10 keV. As a result, the fast neutrons found far from the source are those resulting from high energy neutrons which have not suffered a collision. When these neutrons finally do collide they will be moderated without moving very far from the point of collision. Accordingly, a fair representation of the source of thermal neutrons which can be used as the source term in the diffusion equation is the "first scattering source" [10] which for a point source is given by

$$q(r) = \frac{S}{4\pi r^2} \Sigma_s e^{-\Sigma_s r} .$$

This equation gives the density of first scattering collisions at distance r from an isotropic point source emitting S fast neutrons/sec in an infinite medium. The parameter Σ_s is the macroscopic scattering cross section of the fast source neutrons. The reciprocal of Σ_s is known as the relaxation length, b, defined as the distance the neutron density is reduced by a factor 1/e of its initial value due to scattering. Replacing Σ_s by 1/b, the source term can be written

$$q(r) = \frac{K_1 e^{-r/b}}{r^2} \tag{18}$$

where $K_1 = \frac{S}{4\pi} \Sigma_s$, a constant.

At large r, therefore, the principal variation in the slowing down density arises from a simple exponential decrease combined with the inverse square characteristic of a point source. Moreover, q(r) is not a function of age, τ_T, since every neutron is presumed to slow down fully at its first collision.

The thermal diffusion equation for the one-group approximation can now be written as

$$\nabla^2 \phi_T(r) - \frac{\phi_T(r)}{L_T^2} + \frac{K_1 e^{-r/b}}{\bar{D} r^2} = 0 \tag{19}$$

To satisfy the boundary condition that $\phi_T(r)$ go to zero as $r \to \infty$, the homogeneous solution becomes

$$\phi_T(r)_H = \frac{K e^{-r/L_T}}{r} . \tag{20}$$

A particular solution is then assumed of the form

$$\phi_T(r)_P = \frac{C_1 e^{-r/b}}{r} + \frac{C_2 e^{-r/b}}{r^2} . \tag{21}$$

By substituting this expression into Equation (19), the constants C_1 and C_2 are found to be

$$C_1 = 0$$

and

$$C_2 = \frac{K_1 b^2 L_T^2}{L_T^2 - b^2} \tag{22}$$

The general solution to Equation (19) can now be written

$$\phi_T(r) = \frac{K e^{-r/L_T}}{r} - \frac{K_1 b^2 L_T^2 e^{-r/b}}{\bar{D} r^2 (L_T^2 - b^2)} . \tag{23}$$

If the diffusion length, L_T, is larger than the relaxation length, b, the first term of Equation (23) dominates at sufficiently large r, the thermal flux decays exponentially, and L_T can be evaluated in a simple routine manner. This is the conventional method of determining L_T.

The relaxation length, however, depends on the initial energies of the neutrons generated by the source. Fast

neutrons from a Pu-Be source have relaxation lengths of about 10 cm. in water [11] which exceed 2.78 cm., the corresponding diffusion length of thermal neutrons [6]. Consquently, the thermal flux decays in a more complicated way and the simple theory for the case of a completely thermalized neutron field does not apply. The determination of L_T in water can, however, still be accomplished by measuring both the migration area and the neutron age. From Equation (16) the diffusion length is then obtained from the relation

$$L_T = (M_T^2 - \tau_T)^{\frac{1}{2}} \tag{24}$$

C. DETERMINATION OF NEUTRON AGE

The neutron age, τ, between two energies is proportional to the mean square distance travelled by a neutron as it is being slowed down from the higher to the lower energy. Denoting this distance by $\bar{r}_s^2$, the second spatial moment of the slowing down density can be written as [9]

$$\bar{r}_s^2 (E_0,E) = \frac{\int r^2 q(r,\tau(E_0,E))dv}{\int q(r,\tau(E_0,E))dv} = 6\tau(E_0,E) \tag{25}$$

where E_0 is the energy of the neutron at its point of birth as a fast neutron and E is a lower energy attained as a result of the slowing down process; dv is the volume element, and q is given by Equation (17). Neutron age is now defined by the relation [9]

$$\tau(E_0,E) = \frac{\bar{r}_s^2}{6} (E_0,E) \tag{26}$$

Equation (25) applies to neutrons of any energy and, hence, of any age. In actual measurements, however, the

terminal age is fixed by the resonance energy of the detecting foil. Consequently, in determining the age to thermal energies, τ_T, the spatial distribution of the slowing down density at some energy above thermal is obtained and then a correction is applied to account for the additional age required to reach the thermal region.

The slowing down density of source neutrons at 1.45 eV can be determined by activating cadmium-covered indium foils placed at various distances from the source. The principal indium isotope, IN^{115}, has a strong, isolated absorption resonance at 1.45 eV while the absorption cross-section of cadmium is large below 1.45 eV, but small at higher energies. The cadmium cover, therefore, prevents thermal neutrons from reaching the indium foil; whereas the large indium resonance at 1.45 eV is primarily responsible for any neutron induced activation.

The saturation activity of a cadmium covered indium foil, A_{CD}, is equal to the rate of production of IN^{116} nuclei and can be written as [9]

$$A_{CD} = V \int \phi(r,E)\, \Sigma_{a_{IN}}(E)\, dE \qquad (27)$$

where V is the volume of the foil, $\Sigma_{a_{IN}}$ is the macroscopic absorption cross-section of IN^{115}, and the integral is evaluated across the 1.45 eV resonance. The number of neutrons per cm^3/sec which slow down past a given energy, E, in the diffusion approximation, is given by

$$q(r,E) = \phi(r,E)\xi\, \Sigma_s(E)E \qquad (28)$$

where $\phi(r,E)$ is the energy dependent neutron flux, $\Sigma_s(E)$ is the macroscopic scattering cross-section, and ξ is the

average logarithmic energy decrement. From Equation (28) it follows that

$$A_{CD} = V \int \left[\frac{q(r,E)\ \Sigma_{a_{IN}}(E)}{\xi\ \Sigma_s(E)} \right] \frac{dE}{E} \qquad (29)$$

Assuming that $q(r,E)$, ξ, and $\Sigma_s(E)$ are constant over the small energy range of the resonance peak, this can be written

$$A_{CD} = \frac{Vq(r,1.45)}{\xi\ \Sigma_s} \int \Sigma_{a_{IN}}(E)\ \frac{dE}{E} \qquad (30)$$

That is, the slowing down density at 1.45 eV is proportional to the experimentally measured activity of the foil. By substituting this result into Equation (25), and noting that $dv = 4\pi r^2 dr$, the expression for the age to indium resonance in spherical coordinates is

$$\tau_{IN} = \frac{\bar{r}_s^{\,2}}{6} = \frac{1}{6} \frac{\int_0^\infty r^4 A_{CD}\ dr}{\int_0^\infty r^2 A_{CD}\, dr} \qquad (31)$$

Thus, by knowing only the relative values of $q(r, 1.45)$, the age to 1.45 eV can be obtained by numerically evaluating the integrals in Equation (31). In this analysis the slowing down density is assumed to be approximated by Equation (18).

Another method for measuring neutron age [6], which provides only a rough estimate in hydrogeneous media, is based on the spatial distribution of neutrons of a given

energy described by Equation (17). Taking the logarithms of this equation and considering indium resonance energy leads to

$$\ell n\ q(r) = \text{const} - r^2/4\tau_{IN} \ . \qquad (32)$$

Since the resonance activation is proportional to q(r), a plot of $\ell n\ A_{CD}$ measured at various points from the source can be made. For moderators which satisfy the continuous slowing down theory of the Fermi Age model (e.g. graphite) the experimental points will lie on a straight line. For water, however, the points will lie above a straight line except in a very narrow band about 20 cm. from the source [12]. This is due to the unusual nature of the hydrogen scattering cross-section and the fact that individual neutron energy losses are so large, as previously discussed. In this narrow band, however, an approximate straight line can be drawn whose negative slope will provide an estimate of τ_{IN}.

D. DETERMINATION OF THERMAL MIGRATION AREA

The thermal migration area, defined by Equation (16), correlates with the total mean square distance a neutron travels from its point of birth to its point of capture. This is given by [11]

$$\bar{r}_t^{\,2} = \frac{\int_0^\infty A_S\, r^4\, dr}{\int_0^\infty A_S\, r^2\, dr} \qquad (33)$$

where A_S is the total saturated activity measured as a function of distance r from a point source. Equation (33) can be obtained in a manner analogous to the derivation of Equation (31) for $\bar{r}_S^2$. Here, however, it is the total relative neutron flux which must be known to evaluate the integrals. At energies that activate a bare indium foil, this total flux will be proportional to the saturation activity. Migration area can then be determined from the definition

$$M_T^2 = \frac{\bar{r}_t^2}{6} \tag{34}$$

III. DESCRIPTION OF THE EXPERIMENT

Measurements were made in pure H_2O at 24°C and in mixtures containing 1.16, 8.96, 27.81, 46.65, 70.09 and 80.09 grams of H_3BO_3 per liter of H_2O at 40°C. The last two mixtures contain the highest boron concentrations attained to date.

The experiments were conducted in a cylindrical plexiglass tank, 1.45 ft. in diameter and 4.27 ft. high, which held about 50 gallons of water. This tank was situated atop a smaller, steel tank 2.95 ft. in diameter and 1.25 ft. high, which held about 65 gallons of water. The base tank served to contain the Pu-Be source and also provide a protective water shield. When positioned for measurements in the base tank, the source was 0.625 inches below the base of the plexiglass tank at centerline. A polyethylene jacket 0.125 in. thick made the source holder watertight.

A single steel rod immersed in the tank at the side heated the poisoned mixtures through a rheostat control. This heating rod, plus a continuous running electric stirrer, maintained the medium at a uniform temperature of 104°F (±0.5°).

The relative flux was measured with bare indium foils, 1.0 in. in diameter and .010 in. thick. Foils used in any given measurement had a weight spread of less than 2.65%. Indium resonance activity was measured with the same foils

placed in cadmium covers 0.025 in. thick. A plexiglass foil holder arrangement provided accurate spacing of the foils in the medium on a line perpendicular to the source. The distance between adjacent foils was 0.50 inches for all measurements. Figure 2 shows the experimental apparatus and set-up.

Nine foil positions wereused for each measurement. The closest measuring position to the source was 8.26 cm. while that furthest away was 18.41 cm. Counts of the cadmium covered foils became insignificant beyond this last position.

The cadmium-covered and bare indium foils were irradiated separately during each experiment for a minimum of 8 hours. After irradiation the indium was allowed to decay for 3 minutes to avoid interference with the desired 54-minute activity from the 13 second half life of IN^{116} [11]. The activity of the foils was then counted from each side for 10 minutes; the relatively long counting time having been chosen to improve statistics. The counting system consisted of an end-window Geiger Mueller tube contained in a lead shielded housing, and an electronic scaling unit. This apparatus is summarized in Table 2 and pictured in Figure 3.

Counter background was measured repeatedly during each run as an erratic line voltage perturbation appeared at infrequent intervals. Only rarely was the background stable within statistics for an entire run. The resulting

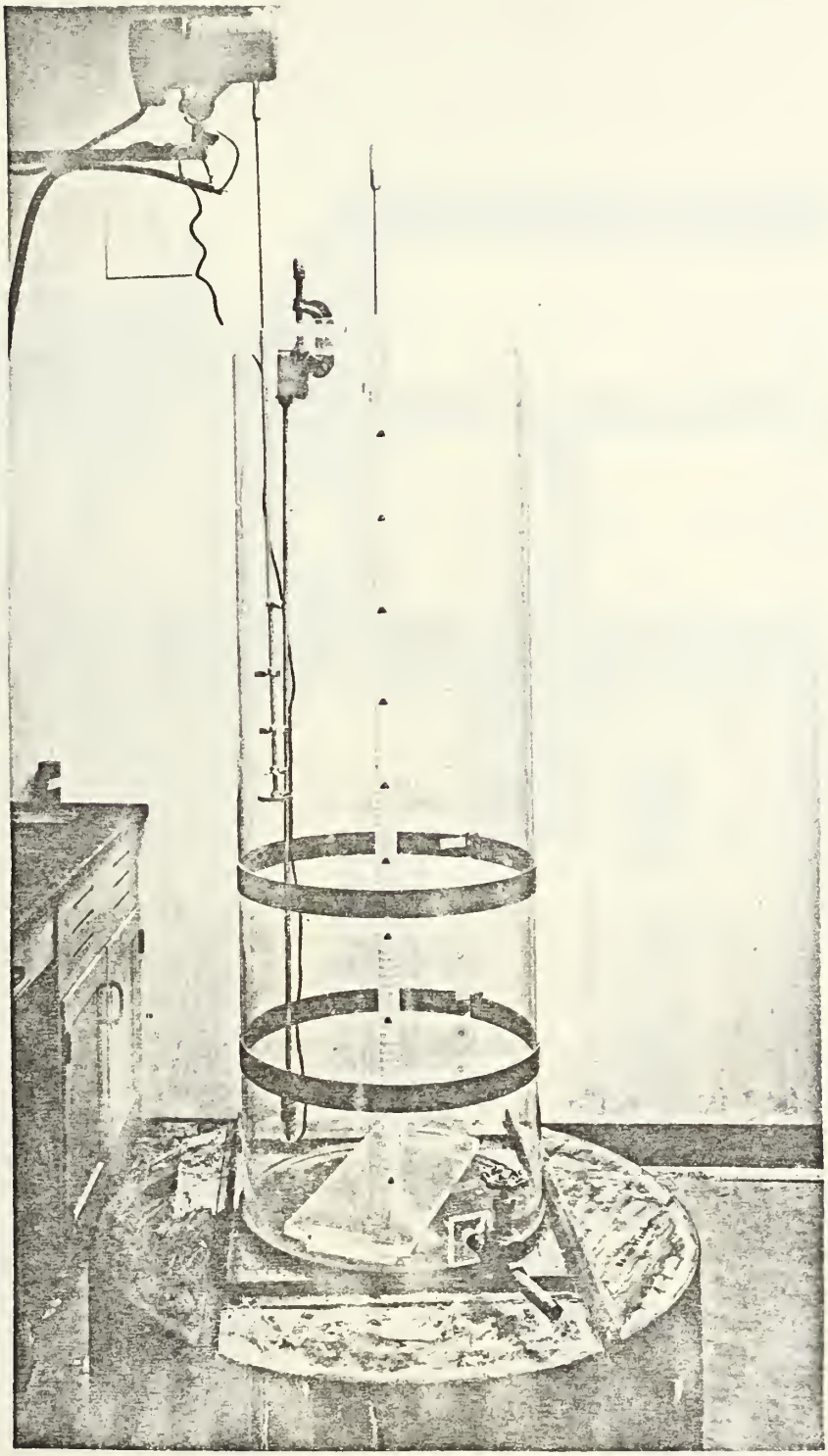

Experimental Apparatus

Figure 2

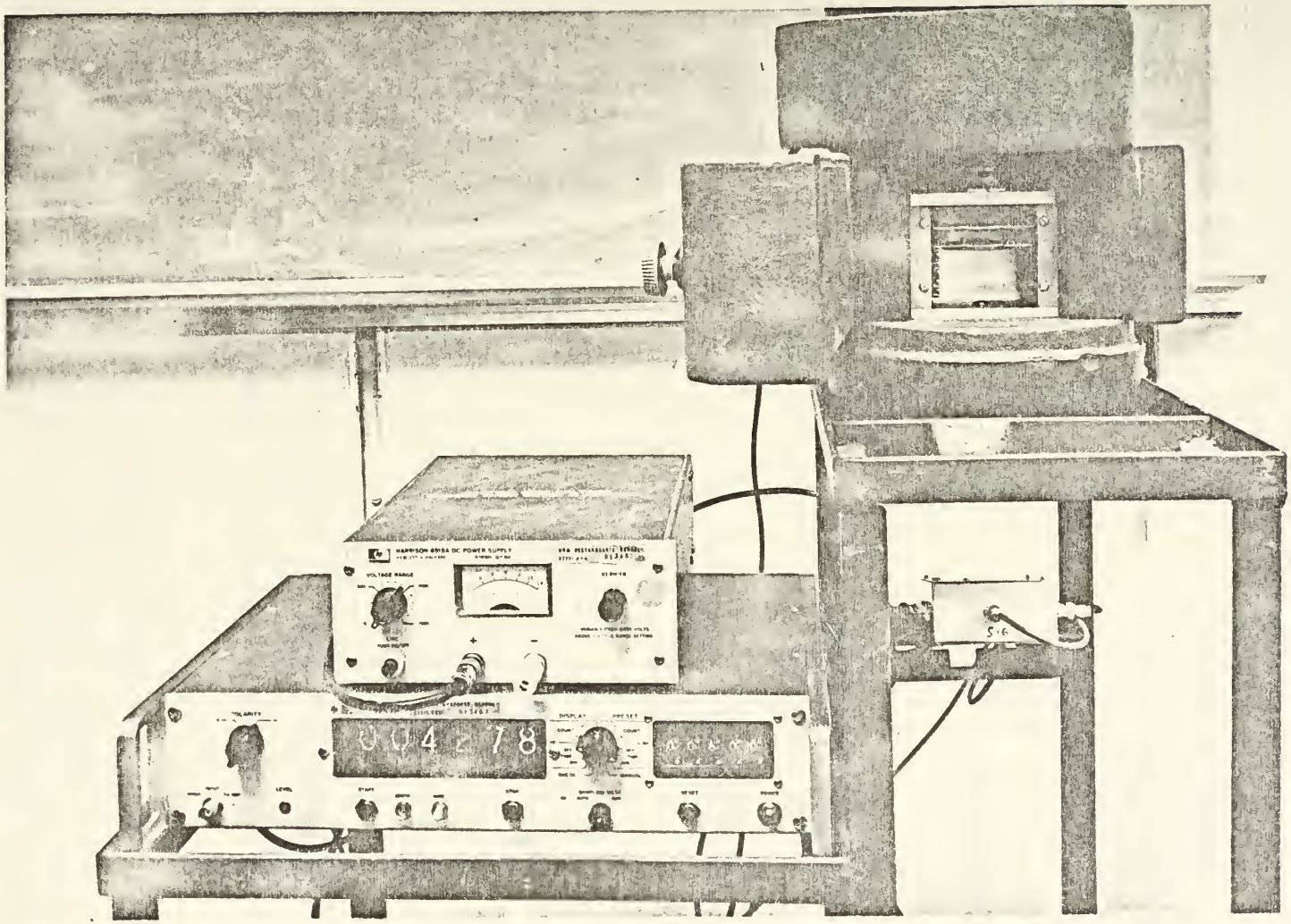

Counting Equipment

Figure 3

TABLE 2

DETECTION EQUIPMENT

Counter	
Activity Detected	Beta and Gamma
Type	Organically-quenched GM
Shape	Cylindrical
Counting Gas	Helium
Manufacturer	Atomic Accessories, Inc.
Amplifier	
Type	Non-overloading
Sensitivity	10 mV
Manufacturer	Hewlett Packard
Model	5554A
Scaler-Timer	
Manufacturer	Hewlett Packard
Model	5201L

necessity for interpolating between background determinations represents one important possibility for nonrandom errors in the results.

Prior to each poison experiment samples of the solution were chemically analyzed for boric acid content. The method of analysis was boric acid titration with glycerine which is outlined in Appendix A.

IV. ANALYSIS OF DATA

A. DETERMINATION OF SATURATED ACTIVITY

Three corrections were applied to the foil data. The first was an internormalization based on foil weight, the second corrected for absorption of indium resonance neutrons by the cadmium cover; and the third corrected for counter resolving time.

The weights of the indium foils used in all measurements varied from 0.9282 to 0.9621 grams. All foil weights were therefore normalized to a weight of 1.0 gram and the resulting corrections applied to the foil counts. The highest value of the weight correction factors obtained in this manner was 1.082.

The indium resonance counting-rate correction was determined to be 1.11. This value was obtained from a curve of correction factor vs. indium foil thickness constructed for a cadmium thickness of 0.025 in. as outlined by Tittle [14].

A number of determinations of counter resolving times were made by following the decay of 54 minute IN^{116} over three hours. An average value of 400 μ sec. was obtained by solving

$$\frac{A_1}{1 - N_1 t} = \frac{A_2}{1 - N_2 t}$$

where A is the extrapolated activity, N is the mean counting rate, and t is the resolving time. A correction factor of 1/(1-Nt) was then applied to all counting runs.

The effect of foil activation by source neutrons above resonance was considered negligible as the closest measurement point was greater than 8 cm. from the source [12]. Also, to insure that the close spacing between foils did not contribute error due to shadowing, activations were made in pure water using various spacing intervals.

After correcting the foil count as described above, the saturated activity in counts per minute was calculated from the equation

$$A_S = \frac{\lambda C}{(1 - e^{-\lambda t_1})(e^{-\lambda(t_2 - t_1)} - e^{-\lambda(t_3 - t_1)})}$$

where C is the total count less background, λ is the disintegration constant of IN^{116}, t_1 is the irradiation time, $t_2 - t_1$ is the waiting time and $t_3 - t_1$ is the waiting time plus counting time [13]. An average quantity was then obtained from the values of A_S computed for each foil side. The computer program used in this calculation is included in Appendix F. Appendix I provides tables of the computed data for all runs.

B. DETERMINATION OF RELAXATION LENGTH

It was pointed out in Section II-B that in hydrogeneous media, the slowing down density at large distances from the source can be approximated by the expression

$$q(r) = \frac{K_1 e^{-r/b}}{r^2} \tag{18}$$

where b is the relaxation length of the fast source neutrons. Since in the framework of age-diffusion theory, the flux is proportional to the slowing down density at a fixed energy, it follows that the cadmium-covered activity at large distances from the source would have the same space dependence described by Equation (18), namely

$$A_{CD}(r) = \frac{K e^{-r/b}}{r^2} \tag{35}$$

To evaluate b from the corrected data, the product $A_{CD}r^2$ was plotted against r on semi-log paper. This plot showed the spherical space distribution beginning to decrease exponentially at about r = 12.5 cm. The distribution for r > 12.5 cm was then fitted, by least squares, with functions of the form of Equation (35); specifically

$$\ell n\ A_{CD}r^2 = \text{const} - r/b \tag{36}$$

The distribution for r > 12.5 cm consisted of only five data points which, for most runs, exhibited large statistical variation due primarily to the low foil activity in this range. Accordingly, the solution resulting from fitting (36) to this data provided only a rough value of the parameter b. A more accurate determination was made by comparing A_{CD} distributions calculated from Equation (35) (using

neighboring values of b) with the measured distribution on a large scale semi-log plot of A_{CD} vs. r. Unlike the $A_{CD}r^2$ spherical space distribution all data on the A_{CD} vs. r plot decreased in value with increasing r; this permitted use of the more reliable data close to the source to indicate which, if any, of the data at r > 12.5 cm were inconsistent with the decreasing trend of the overall distribution. After discarding any poor data indicated by this procedure, the calculated A_{CD} distributions were normalized and fitted to the measured distribution for r > 12.5 cm until the closest possible fit was attained. The value of b used in calculating the distribution found to give the closest fit became, then, the negative reciprocal of the slope of the exponential portion of the $A_{CD}r^2$ vs. r curve.

The above procedure was also used to determine relaxation length for the bare foil activity (A_S) and, thus, the slope of the A_Sr^2 vs. r curve. Foster, in measuring the age of Na-Be neutrons [15], assumed no loss in precision from using the same value of b for both the A_{CD} and A_S distributions. The present procedure, however, clearly showed a small difference in the two, the b for the resonance distribution being less in every case, as it should. The work of Rush with Ra-Be neutrons [16] showed this same tendency. Figure 4 is a plot of A_{CD} vs. r and A_S vs. r for the pure water run which includes the data computed from Equation (35), normalized to the experimental data. Figure 4 also shows the marked deviation between

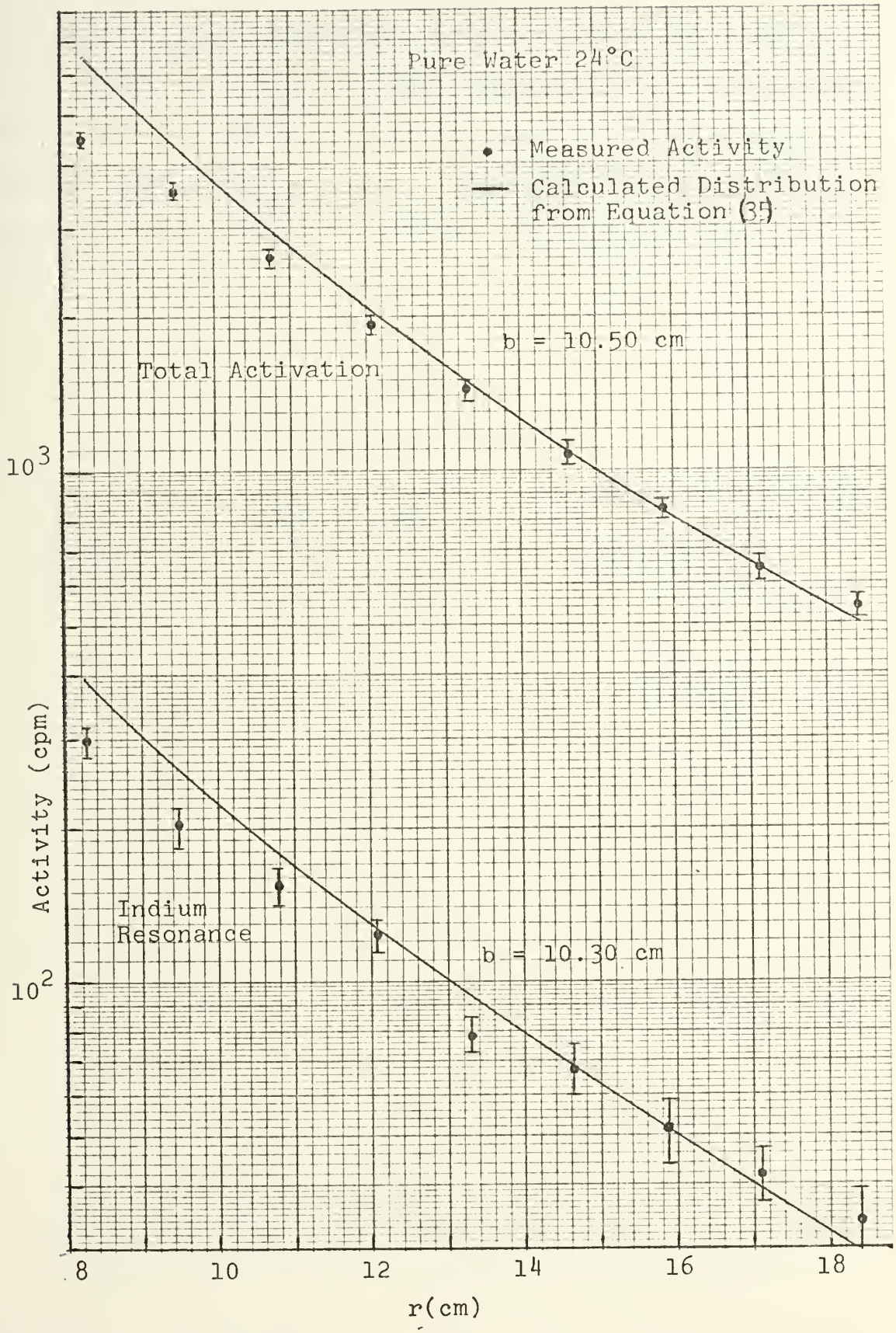
Pure Water 24°C
Measured Activity
Calculated Distribution from Equation (35)
b = 10.50 cm
Total Activation
b = 10.30 cm
Indium Resonance
Activity (cpm)
10^3
10^2
8
10
12
14
16
18
r(cm)

Figure 4

the computed and experimental data for points near the source. This is to be expected since Equation (35) applies only at larger distances from the source. Similar plots for the poisoned water runs are presented in Appendix B. The values of b determined for all experimental runs are given in Table 3.

TABLE 3

RELAXATION LENGTH

Boric acid (g/ℓ)	b(±0.03 cm) Indium Resonance Activation	b(±0.02 cm) Total Activation
- - -	10.30	10.50
1.16 ± .17	10.25	10.45
8.96 ± .36	10.25	10.38
27.81 ± .79	10.22	10.36
46.65 ± 1.2	10.19	10.35
70.09 ± 1.3	10.15	10.35
80.09 ± 1.9	10.15	10.35

C. DETERMINATION OF AGE AND MIGRATION AREA

A smoothed curve was drawn through data points less than $r = 12.5$ cm. on the $A_{CD}r^2$ and $A_S r^2$ versus r plots. For $r \triangleright 12.5$ cm. the data were extrapolated to infinity by means of a straight line having a slope equal to the negative reciprocal of the parameter b. The areas under the smoothed

curves were found by integrating the straight-line portions analytically and by using Simpson's Rule for the remainder. Points from these curves were used to obtain the curves $A_{CD}r^4$ and $A_S r^4$ versus r. These latter curves were found to approach straight lines beyond r = 45 cm. and areas were calculated accordingly. After the area under each of the four curves had been determined, the second moments $\bar{r}_S^2$ and $\bar{r}_t^2$ were obtained from Equations (25) and (33). The neutron age to indium resonance and total migration area then followed from Equations (31) and (34). The computer program used in these computations is included in Appendix G. Figures 5 and 6 are plots of $A_{CD}r^2$, $A_S r^2$, $A_{CD}r^4$, and $A_S r^4$ versus r for pure water. Plots of $A_{CD}r^2$ and $A_S r^2$ versus r for the poisoned experiments are given in Appendix C.

Table 4 gives the values of τ_{IN} and M_T^2 determined for all experiments. The errors cited have been estimated from $A_{CD}r^2$ and $A_S r^2$ versus r plots by using the individual, unaveraged foil points to construct maximum and minimum values for τ_{IN} and M_T^2 [11].

A rough check on the experimentally determined values of age was made by following the procedure discussed in Section II-D with Equation (32). Values of activity as a function of r had been previously computed from Equation (35) in determining the closest value of relaxation length to fit the experimental points. This data was plotted on semilog paper against r^2. A narrow band between r = 18 and r = 22 cm. presented the closest straight line

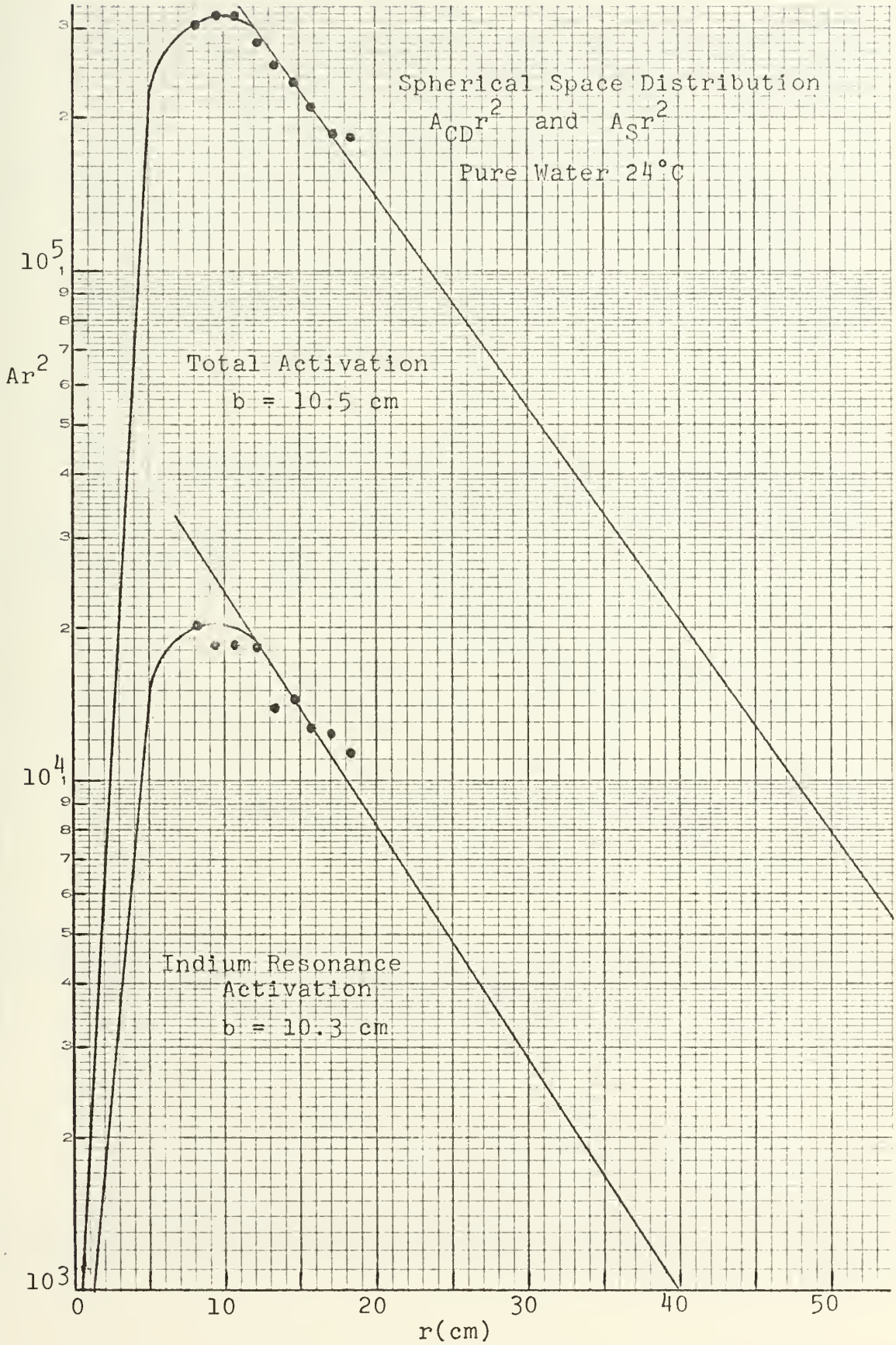
Spherical Space Distribution
$A_{CD}r^2$ and $A_S r^2$
Pure Water 24°C
Total Activation
b = 10.5 cm
Indium Resonance
Activation
b = 10.3 cm
Ar^2
10^5
10^4
10^3
0
10
20
30
40
50
r(cm)

Figure 5

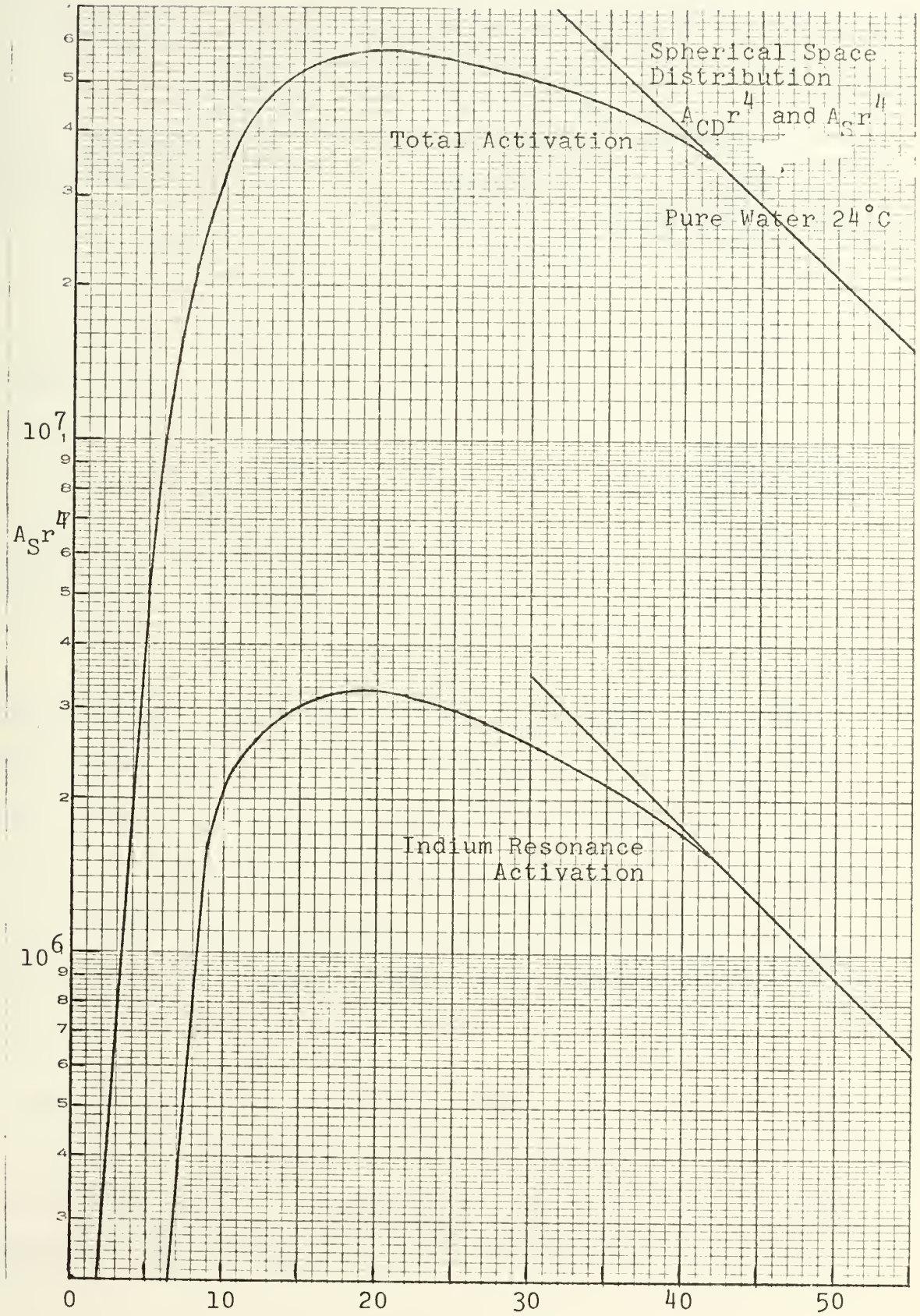
Spherical Space Distribution
$A_{CD}r^4$ and A_Sr^4
Total Activation
Pure Water 24°C
Indium Resonance Activation
A_Sr^4
10^7
10^6
0
10
20
30
40
50

Figure 6

TABLE 4

MIGRATION AREA AND NEUTRON AGE

Boric Acid g/ℓ	M_T^2 (cm^2)	τ_{IN} (cm^2)	τ_{IN} (cm^2) (From Eq. (32))
- - -	61.76 ± 1.84	52.19 ± 0.79	51.75
1.16 ± .17	59.41 ± 0.68	52.06 ± 2.34	51.62
8.96 ± .36	55.63 ± 1.17	52.02 ± 3.18	51.62
27.81 ± .79	54.21 ± 2.89	51.96 ± 3.06	51.55
46.65 ± 1.2	53.47 ± 3.13	51.29 ± 3.42	51.47
70.09 ± 1.3	53.37 ± 1.57	51.26 ± 3.11	51.37
80.09 ± 1.9	53.13 ± 3.13	51.20 ± 4.21	51.37

approximation. The slope of this line, equal to $-\frac{1}{4\tau_{IN}}$ from Equation (32), was then determined by the method of least squares. A plot of A_{CD} vs. r^2 for pure water with b = 10.3 is provided in Appendix D. Table 4 includes values of τ_{IN} obtained in this manner for all experimental runs. The least square machine program used in this determination of age is included in Appendix H.

D. DETERMINATION OF DIFFUSION LENGTH

Prior to determining L_T from Equation (24), it was necessary to apply a correction to τ_{IN} to account for the additional age required to reach the thermal energy of 0.025 eV.

Estimates of this correction for hydrogeneous media are found in the literature ranging form 0.3 cm^2 [17] to 1.8 cm^2 [11], the latter value being that used by Valenti for measurements with a Pu-Be neutron source. In this investigation it was found that adding a correction of 1.8 cm^2 to the value of τ_{IN} determined for pure water yielded a value of 2.786 for L_T. This is in excellent agreement with published results obtained by the more conventional method of measuring the exponential attenuation of thermal neutrons. It was also noted that 2.786 cm was in precise agreement with the value of L_T obtained from the empirical equation [14]

$$L_{T_{H_2O}} = 2.64 + 0.0061\ T \text{ cm} \qquad (37)$$

for a temperature, T, of 24°C. Accordingly, a correction of 1.8 cm^2 for the age from indium resonance to thermal energies was applied to the experimentally determined value of τ_{IN} for all runs and L_T was then computed from Equation (24). Results are presented in Table 5. Errors have been estimated from a combination of those previously cited in Table 4 for τ_{IN} and M_T^2.

E. DETERMINATION OF THE THERMAL FLUX DISTRIBUTION ACCORDING TO TWO-GROUP THEORY

A final check on the results obtained for pure H_2O and the poison mixtures was made by computing the thermal flux distribution from Equation (15). The experimentally determined values of L_T and τ_T were used in the equation and the

TABLE 5

MEASURED DIFFUSION LENGTH AT 24°C IN PURE WATER AND 40°C IN POISONED WATER

Boric Acid g/ℓ	L_T(cm)
- - -	2.7862 ± .14
1.16 ± .17	2.3559 ± .15
8.96 ± .36	1.3307 ± .14
27.81 ± .79	0.6664 ± .19
46.65 ± 1.2	0.6213 ± .20
70.09 ± 1.3	0.5594 ± .18
80.09 ± 1.9	0.3640 ± .30

total macroscopic absorption cross-section of the poisoned medium was computed from

$$\overline{\Sigma}_a = \Sigma_{a_{hydrogen}} + \Sigma_{a_{Boron}}$$

where $\Sigma_{a_{hydrogen}}$ was taken to be

$$\Sigma_{a_{hydrogen}} = \Sigma_{a_{H_2O}} + N_{H_3BO_3} \times 3\sigma_{a_{hydrogen}}$$

and

$$\Sigma_{a_{Boron}} = N_{H_3BO_3} \times \sigma_{a_{Boron}}$$

The parameter σ_a is the microscopic absorption cross-section and $N_{H_3BO_3}$ is the number of molecules of H_3BO_3 per cm^3 determined from

$$N_{H_3BO_3} = \frac{\rho_{H_3BO_3} A_0}{\text{Molecular weight}}$$

where ρ is the density in grams/cm^3 and A_0 is known as Avogadro's number, which is 6.024×10^{23} molecules per gram mole.

The computed values of flux were then normalized to the thermal saturated activity which was obtained by subtracting the covered foil from the bare foil data. The results were plotted together on semilog paper and compared. Figure 7 gives this comparison plot for pure water. Similar plots for other runs are contained in Appendix E. Table 6 lists the values of $\overline{\Sigma}_a$ determined for each run together with the maximum deviations found between the experimental data and flux distributions obtained from Equation (15).

TABLE 6

COMPARISON OF EXPERIMENTAL RESULTS WITH SOLUTIONS OF THE TWO-GROUP THERMAL FLUX EQUATION

Boric acid g/ℓ	$\Sigma_a (cm^{-1})$	MAX deviation (%)
- - -	0.0222	11.7
1.16 ± .17	0.0307	14.2
8.96 ± .36	0.0882	12.5
27.81 ± .79	0.2270	7.2
46.65 ± 1.2	0.3657	3.5
70.09 ± 1.3	0.5384	2.3
80.09 ± 1.9	0.6120	- - -

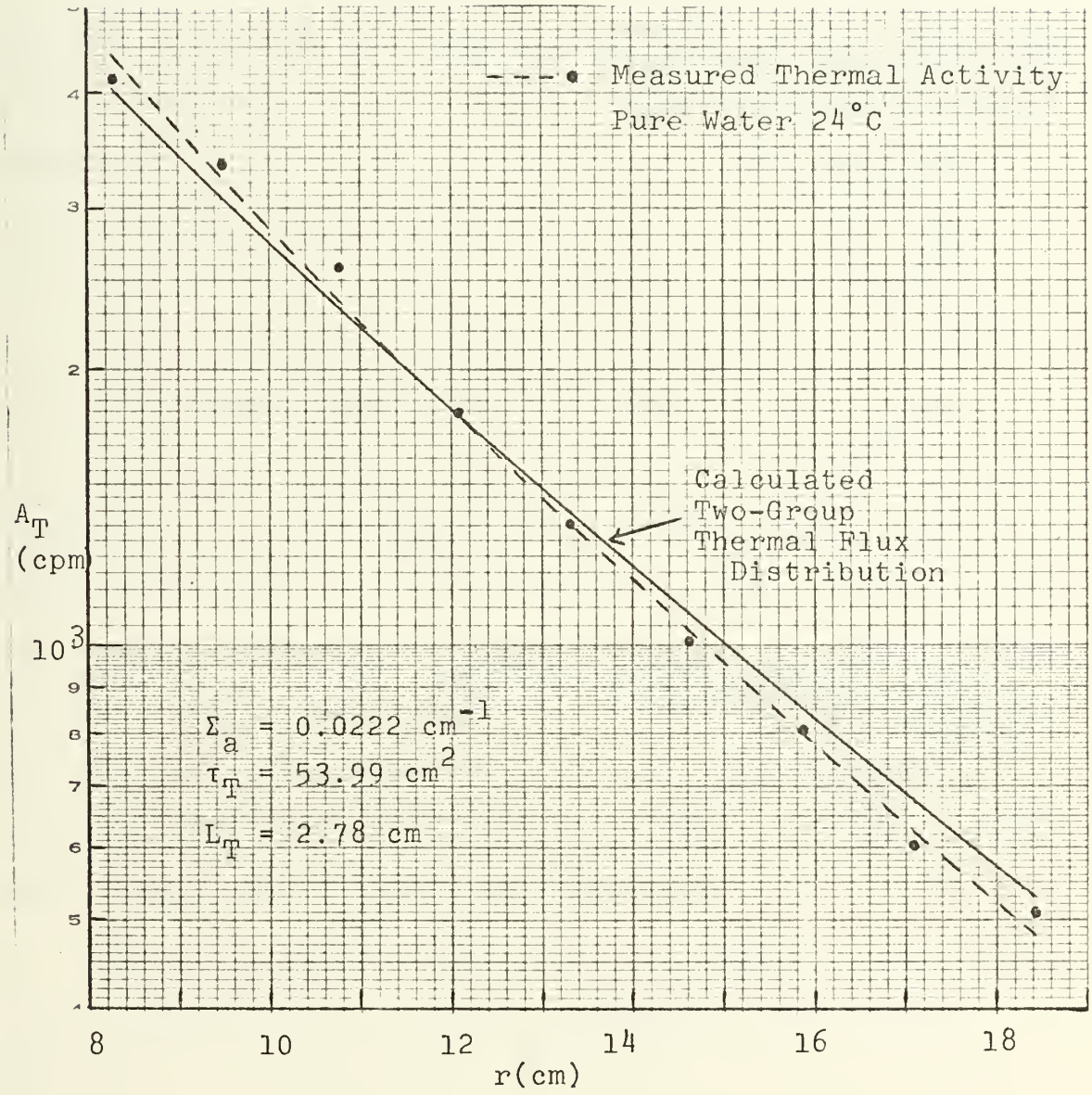
Measured Thermal Activity
Pure Water 24°C
Calculated
Two-Group
Thermal Flux
Distribution
A_T
(cpm)
10^3
$\Sigma_a = 0.0222\ cm^{-1}$
$\tau_T = 53.99\ cm^2$
$L_T = 2.78\ cm$
8
10
12
14
16
18
r(cm)

Figure 7

V. COMPARISON OF RESULTS WITH THEORY AND PREVIOUS EXPERIMENTAL MEASUREMENTS

A. AGE AND THERMAL MIGRATION AREA

Theoretical investigation of the age of fission neutrons in pure H_2O has been extensively pursued and, for this case alone, there exist calculations of the actual slowing down distribution which can be compared in detail with measured distributions. Comparable results have not been obtained for non-fission sources due, primarily, to uncertainties in the energy spectrums. There is no account in the literature of an age calculation for a Pu-Be source. Coveyou and Sullivan [17], however, have calculated the age to indium resonance, τ_{IN}, for monoenergetic sources in H_2O using a Monte Carlo age code which provides a rough comparison for this work. The plotted results of their calculations demonstrate a rapid rise in age with increasing source energy; and for an initial neutron energy corresponding to the average energy of a Pu-Be source (4.2 MeV), these results give a value for τ_{IN} of 52 cm^2 ($\pm$.5 cm^2).

Although clearly defined, thermal migration area, M_T^2, is not amenable to calculation because of theoretical difficulties encountered in describing the scattering of thermal neutrons [18]. As was borne out by this experiment, however, thermal diffusion length is small in highly absorbing systems so that the predominant contribution to M_T^2 comes from the slowing down process. This allows some

comparison of measurements of M_T^2 and calculations of τ_T by treating the thermal diffusion as an additive correction.

The only measurements of M_T^2 and τ_{IN} from a Pu-Be source which have been published to date were those by Valenti and Sullivan for τ_{IN} [19], and by Valenti for M_T^2 [11]. Their results are compared with those obtained in this work in Table 7. A factor which accounts for some of the difference in these two measurements is a source effect correction used by Valenti and Sullivan [19]. This involved a correction to the indium resonance activity to account for the finite size of the source and was intended to approximate a distribution closer to that expected from a point source. Due to the relatively low counting rates encountered in this work, it is estimated that a source effect correction would have increased the activity of the foil nearest the source by less than 1% [11].

TABLE 7

COMPARISON OF RESULTS WITH PREVIOUS EXPERIMENTS
Plutonium-Beryllium Neutrons in Pure Water

	Present Results	Valenti & Sullivan [19]	Valenti [11]
$M_T^2(cm^2)$	61.76 ± 1.84		61.07
$\tau_{IN}(cm^2)$	52.19 ± 0.79	52.8 ± 2.0	

In Figure 8, measured values of the parameters M_T^2 and τ_{IN} are plotted as a function of poison concentration. The differences between the two curves is seen to reflect the 1/v behavior of the boron absorption cross-section. At low thermal energies absorption is heavy and affects only M_T^2; at energies above thermal, absorption falls off rapidly and has a very small affect on both M_T^2 and τ_{IN}.

B. THERMAL DIFFUSION LENGTH

The close agreement between the theoretical value of L_T in pure H_2O at room temperature with that obtained in this experiment was pointed out in Section IV-D.

Previously reported investigations of L_T dependence on the poison concentration of H_2O were conducted using a thermal reactor as a neutron source [3, 4] and a Sb-Be (25keV) source [5]. As a result there existed only a small component of fast-flux in the region of measurement which could easily be eliminated from the experimental data. This permitted relatively straightforward measurements of the exponential attenuation of thermal neutrons as discussed in Section II-C and, consequently, gave final results of high accuracy.

Figure 9 compares the results obtained by Goddard and Johnson [3] with values of L_T found in this experiment. The two sets of data are found to be in good agreement when the 25°C temperature difference is taken into account. Since their results were obtained at 65°C, their values of L_T

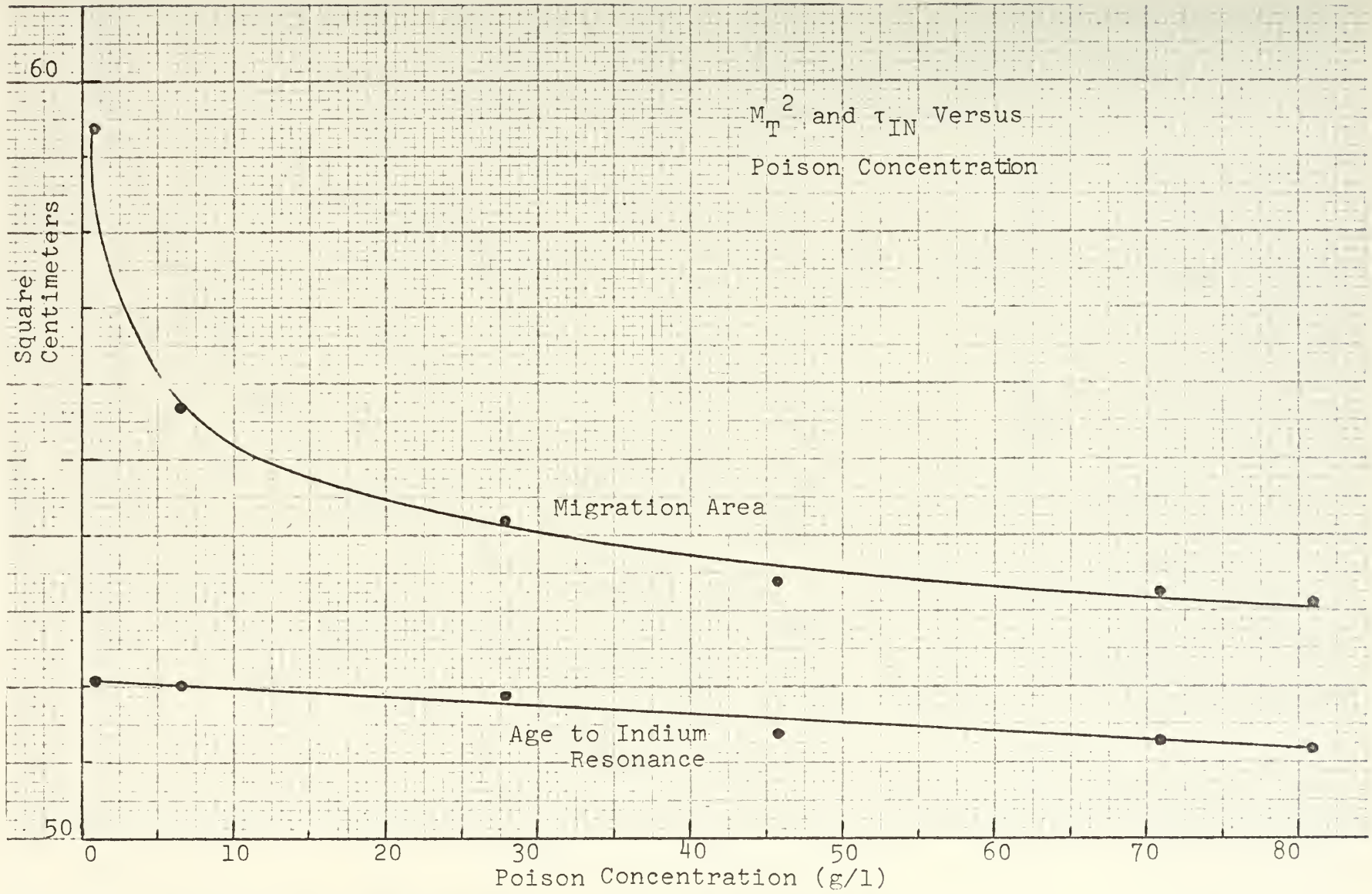
M_T^2 and τ_{IN} Versus
Poison Concentration
Square Centimeters
60
50
Migration Area
Age to Indium Resonance
0
10
20
30
40
50
60
70
80
Poison Concentration (g/l)

Figure 8

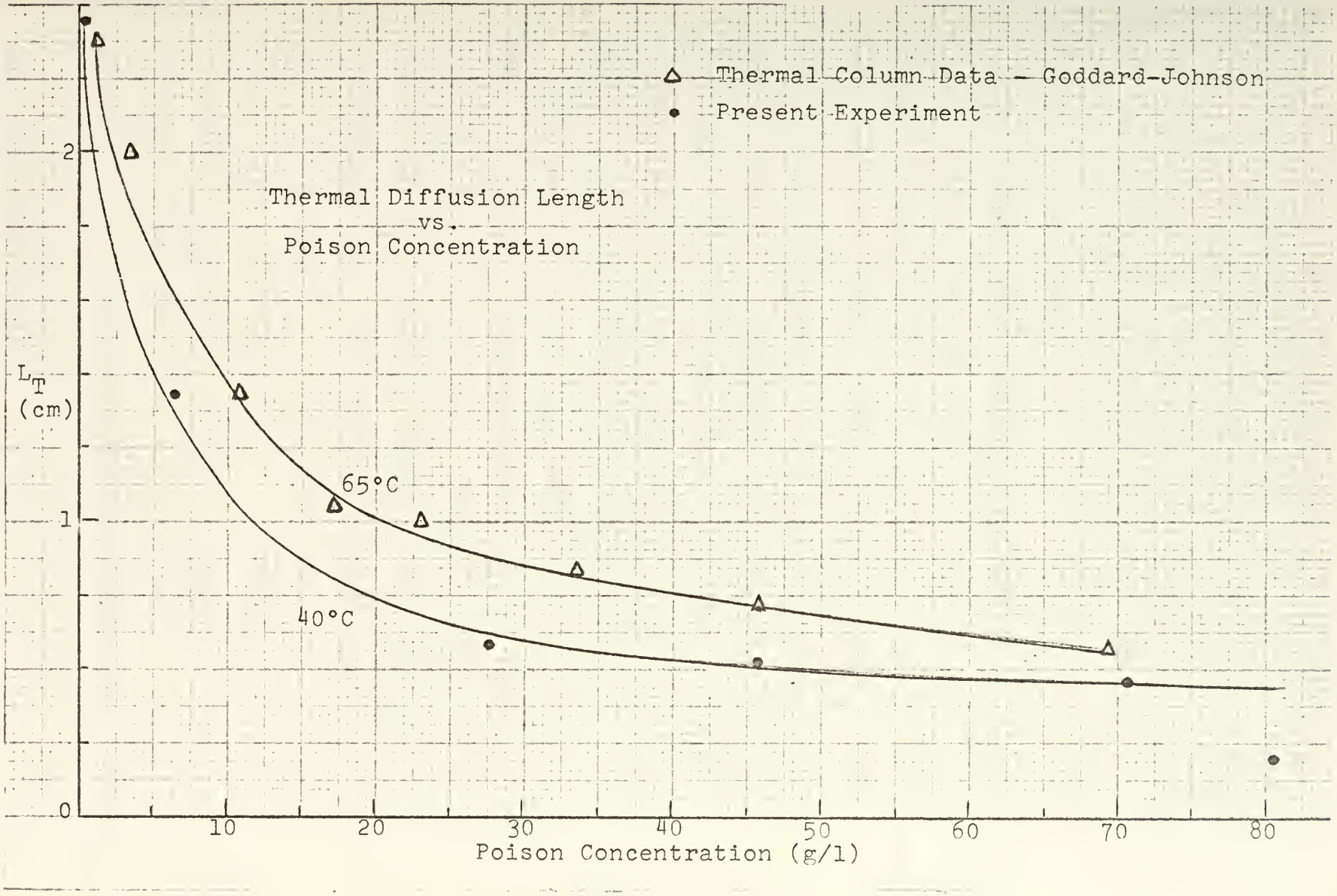
Thermal Column Data — Goddard-Johnson
Present Experiment
Thermal Diffusion Length
vs.
Poison Concentration
L_T (cm)
65°C
40°C
0
1
2
10
20
30
40
50
60
70
80
Poison Concentration (g/l)

Figure 9

should be higher according to Equation (37). It can be seen from the curve representing the present measurements that absorbing solutions with concentrations of 70.09 and 80.09 g/l lay outside the Corngold limit (0.6 cm).

C. TWO-GROUP THERMAL FLUX

The thermal flux computed from Equation (15) is compared with measured values of saturated activity for each experimental run in Figure 7 and Appendix E. Due to the complicated manner in which Pu-Be neutrons slow down, these computations provided the only method of examining initial activity data for agreement with a distribution predicted by theory. It is evident from the maximum deviations given in Table 6 that the measured and calculated distributions come closer in agreement with increasing poison concentration.

The purpose of the experimental set up was to approximate as closely as possible the "infinite medium" condition which was a basic assumption in the theoretical treatment of both age and diffusion length. That there was, in fact, no leakage in the axial direction is deemed a valid conclusion from the absence of detectible bare foil activity beyond 32 cm. from the source. An indication of the extent of lateral leakage was obtained by measuring total activity radially outward from the source in pure H_2O. The extrapolated distance beyond the physical dimensions at which the flux can be assumed to fall to zero was found to be 1.29 cm. This result is displayed in Figure 10 from which it can be

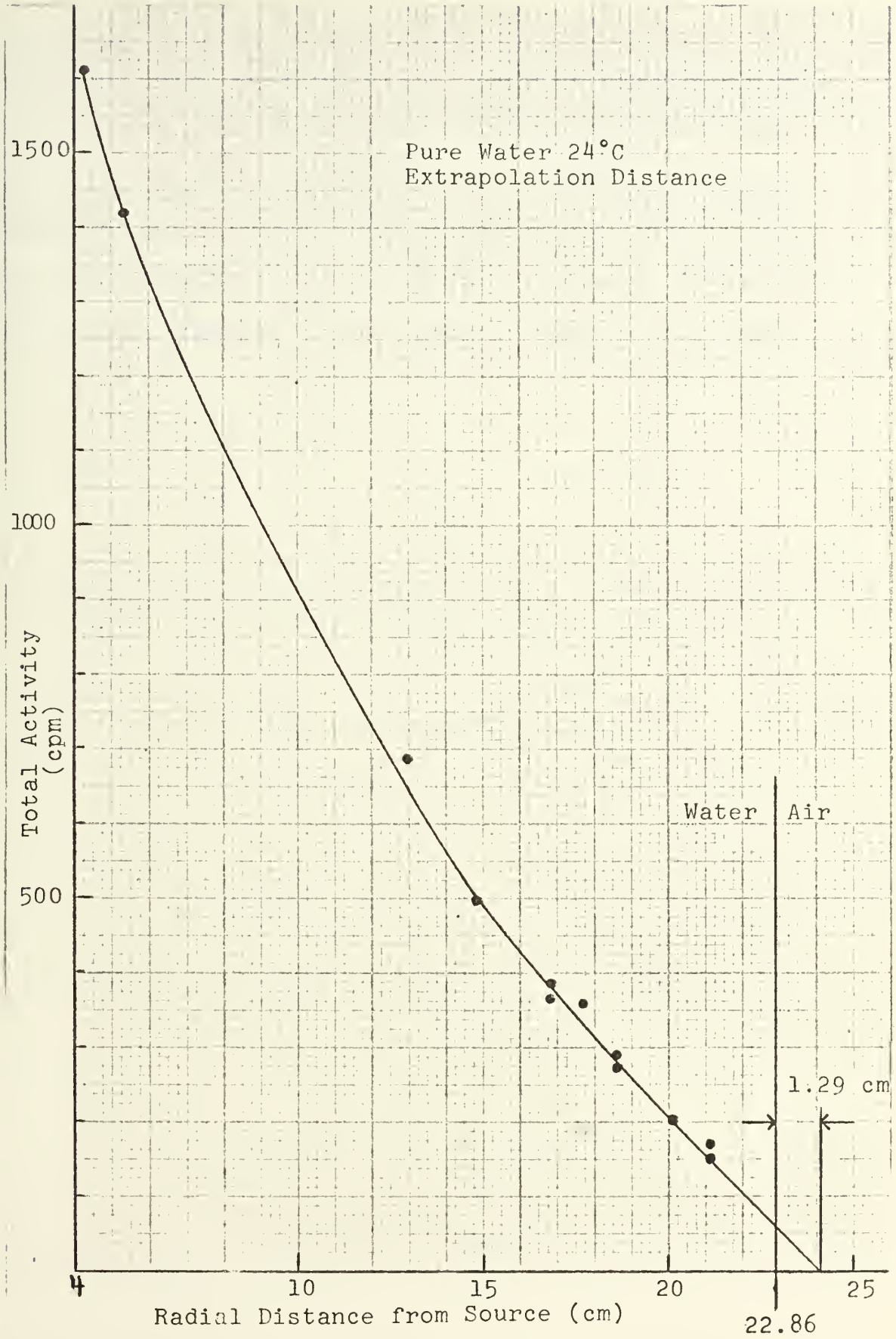
Pure Water 24°C
Extrapolation Distance
1500
1000
500
Total Activity (cpm)
Water
Air
1.29 cm
4
10
15
20
25
Radial Distance from Source (cm)
22.86

Figure 10

seen that even in pure water the "infinite medium" assumption was not seriously violated. The minor differences between the measured and calculated flux distributions for concentrations of 46.65 and 70.09 g/l indicate the betterment of the assumption at the heavier absorber concentration. This is most apparent from a study of the plots in Appendix E.

VI. CONCLUSIONS

The dependence of diffusion length on poison concentration was found to agree well with that reported by Goddard and Johnson [3]. However, because diffusion length as obtained in this experiment is the square root of a small difference between two large numbers, the results given in Table 5 include sizable estimates of error. Errors in the measurements from which diffusion length was obtained were due to limited experimental conditions, the most serious of which was the weak neutron source, resulting in a low activity and a small number of data points. This in turn increases the statistical error.

Previous measurements of neutron age and migration area from a Pu-Be source in pure water [11, 19] agree with the present results within the experimental errors. This report is the first of measurements of these parameters as a function of poison concentration. Accordingly, the results given in Table 4 should be of considerable value in extending our understanding of the slowing down process. The errors associated with each measurement have been conservatively estimated and are meant to serve as bounds on the error, rather than a probable error.

It is evident from the experimental data plotted for the heaviest concentration (80 g/l) that it was impossible to make a reliable age measurement in this case. The value

given for this run is therefore merely a logical estimate based heavily on the previous measurements. It follows from this that the numerical value listed for diffusion length at this concentration is also unreliable. However, since it can be assumed that each of these values approximates the result one would expect to obtain had a measurement been possible, they were used in Equation (15) to calculate a thermal flux distribution. The result of this calculation is plotted in Figure 11 together with the experimental data through which no curve could be drawn. Figure 11 vividly shows the irresolute behavior of the thermal distribution at the 80 g/l boron concentration. It is concluded from this, and from the failure of the age measurement at this concentration, that the "maximum absorption" limit was exceeded in this experiment. The cadmium measurements of Goddard and Johnson together with the present results indicate that the diffusion length corresponding to this limit is about 0.5 cm, slightly less than the theoretical value. The absorption cross-section of the supporting medium at the time the final measurements were attempted was 0.6120 cm^{-1}.

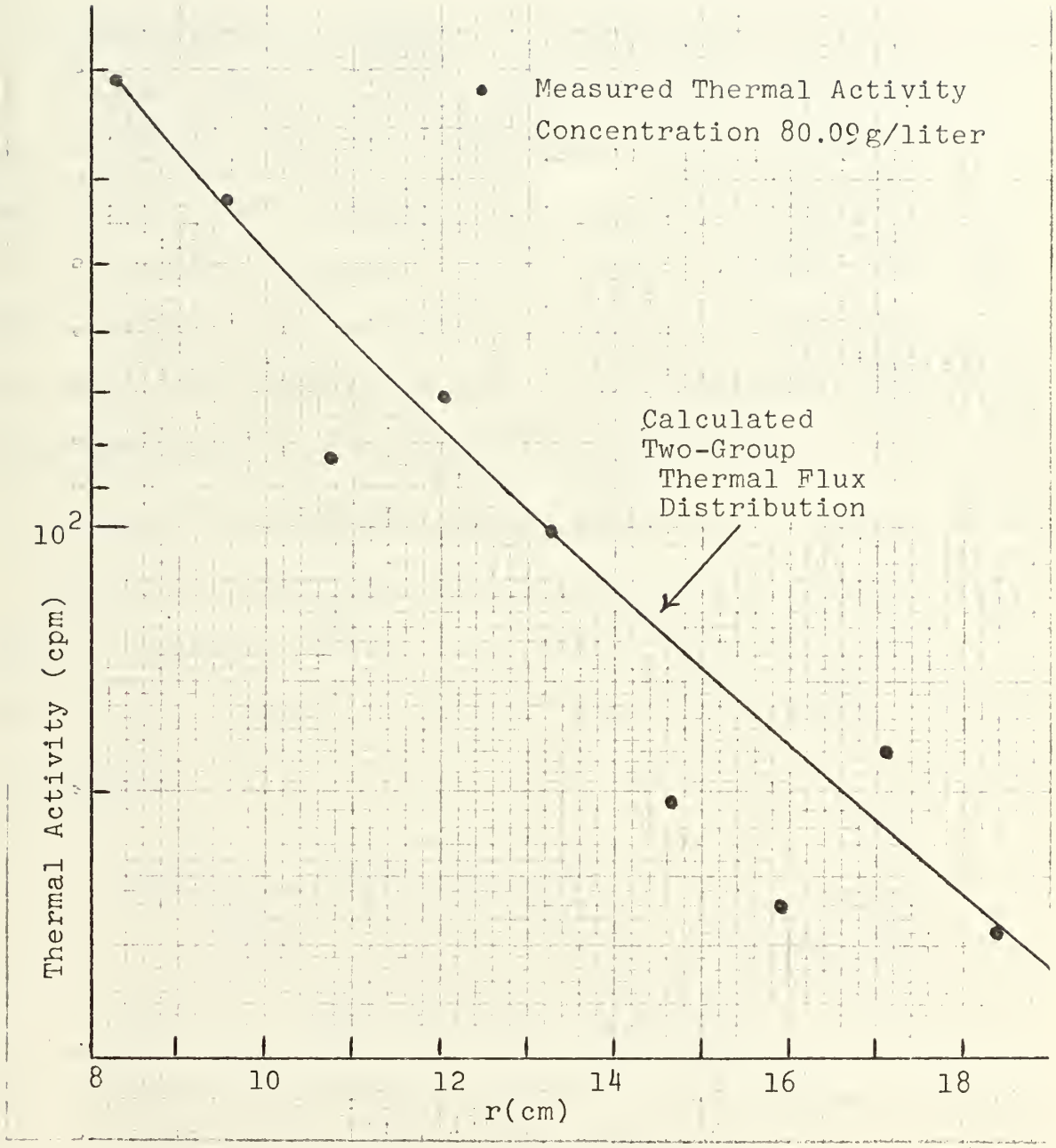
Measured Thermal Activity
Concentration 80.09 g/liter
Calculated
Two-Group
Thermal Flux
Distribution
10^2
Thermal Activity (cpm)
8
10
12
14
16
18
r(cm)

Figure 11

APPENDIX A

METHOD OF CHEMICAL ANALYSIS FOR DETERMINING BORIC ACID CONCENTRATION

A. PREPARATION OF STANDARD

A 1-gram sample of H_3BO_3 (Mol wt 61.84), finely ground, was dissolved in 300 ml of pure H_2O. To this solution in a beaker were added 10 drops of phenolphthalein indicator and 25 ml of neutral glycerol. From a buret, standard NAOH was added dropwise until a distinct reddish-pink color appeared. This marked the true end point for boric acid and established the molarity (Z) of the standard in moles/liter.

B. ANALYSIS OF MODERATOR CONCENTRATION

To 25 ml of moderator solution were added indicator and NAOH as described above. The standard alkali was then added dropwise until the true end point was reached.

C. EXAMPLE

1.33 ml of NAOH produced end point in solution containing 0.162 moles H_3BO_3.

$Z = \frac{.0162}{.00133} = 12.15$ moles/liter <u>standard alkali</u>

0.3 ml of standard alkali produced end point in 25 ml of sample drawn from moderator

(25 ml)(molarity of sample) = (.3 ml)(Z)

molarity of sample = .146 moles/liter

(61.84)(.146) = 9.03 g/l H_3BO_3 <u>concentration of moderator</u>

APPENDIX B

PLOTS OF INDIUM RESONANCE AND TOTAL ACTIVITY VERSUS DISTANCE FROM THE SOURCE FOR POISON RUNS

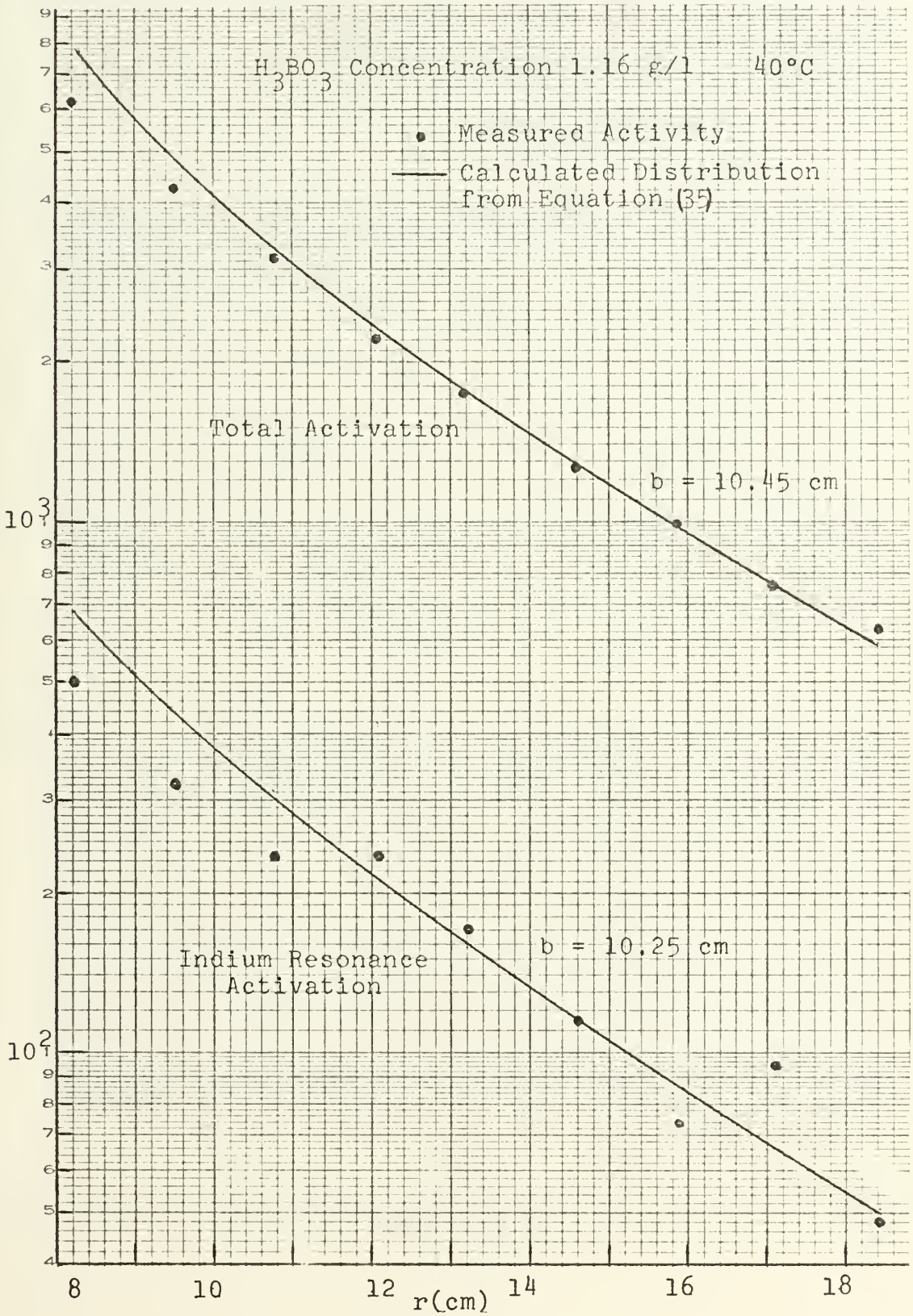

Figure 12

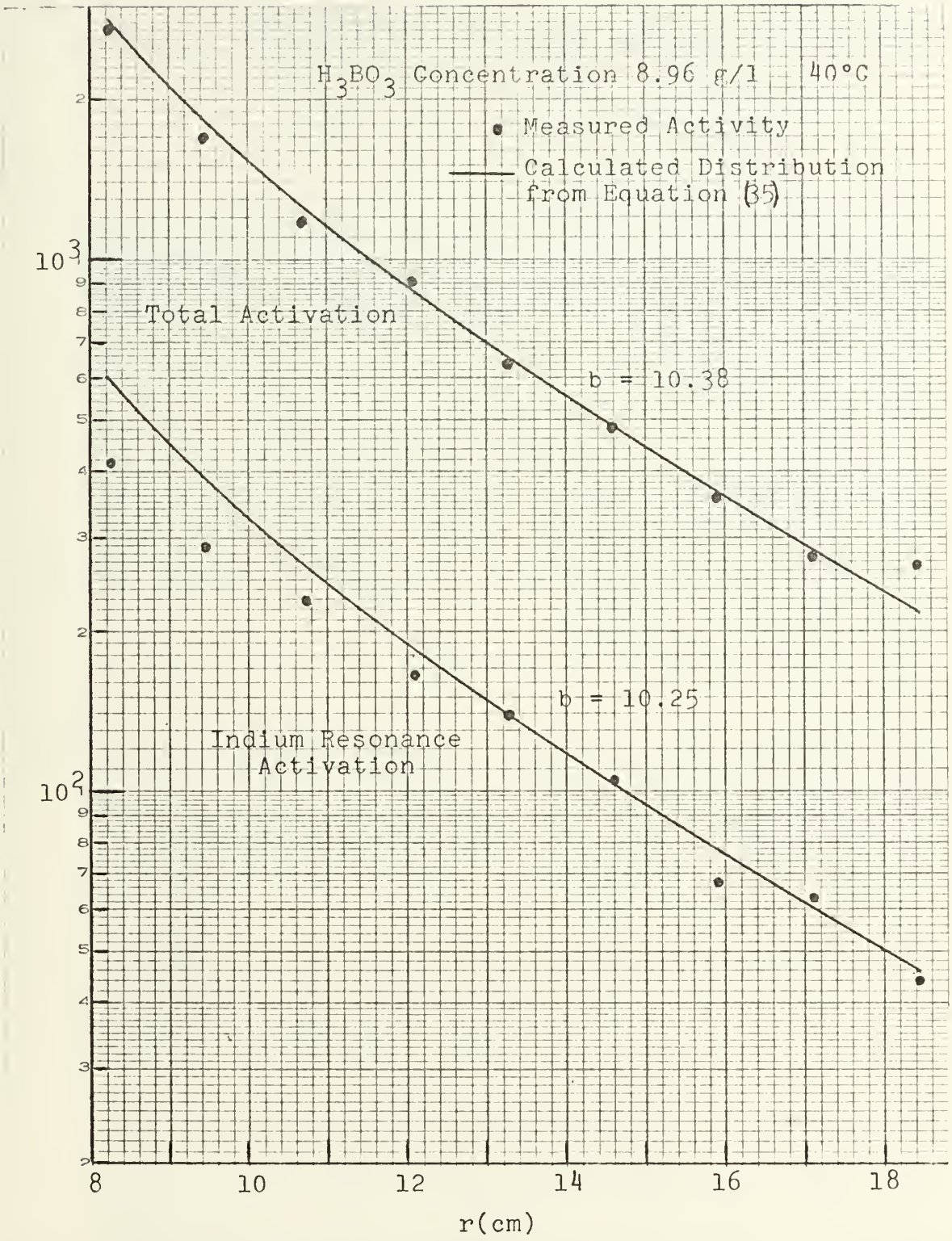
H_3BO_3 Concentration 8.96 g/l 40°C
Measured Activity
Calculated Distribution from Equation (35)
Total Activation
b = 10.38
b = 10.25
Indium Resonance Activation
10^3
10^2
8
10
12
14
16
18
r(cm)

Figure 13

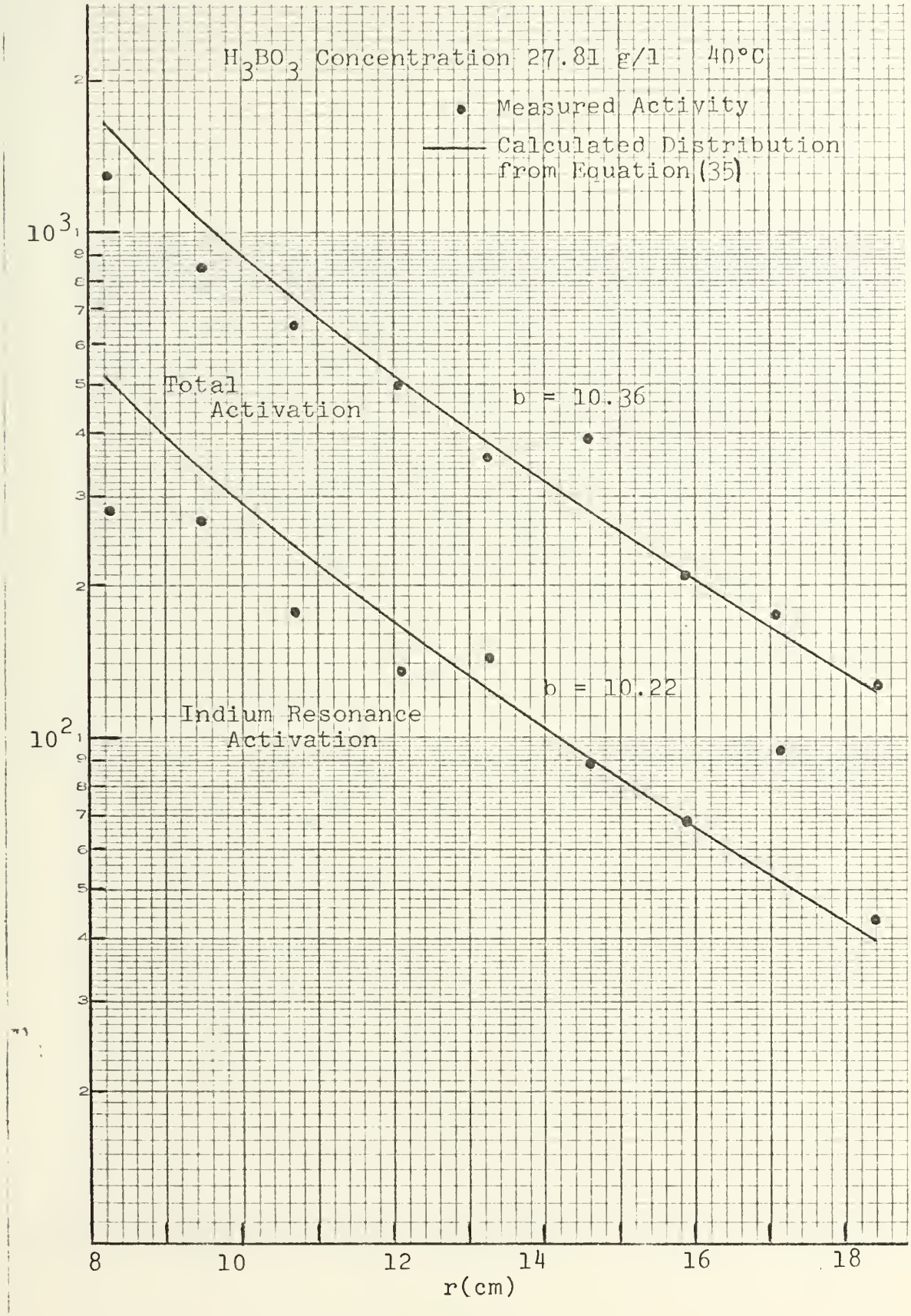
H_3BO_3 Concentration 27.81 g/l 40°C
Measured Activity
Calculated Distribution from Equation (35)
Total Activation
b = 10.36
Indium Resonance Activation
b = 10.22
10^3
10^2
8
10
12
14
16
18
r(cm)

Figure 14

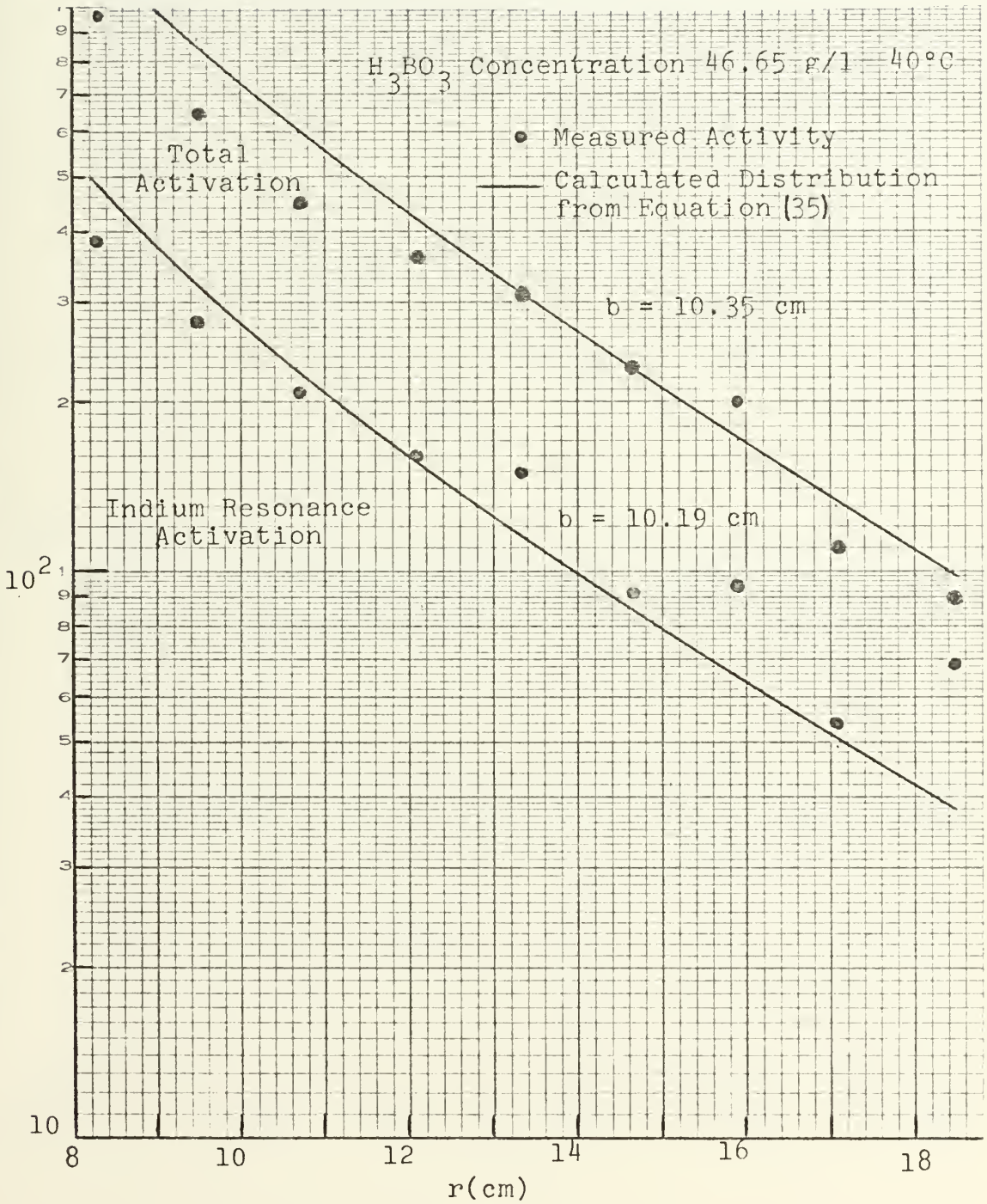
H_3BO_3 Concentration 46.65 g/l 40°C
Measured Activity
Calculated Distribution from Equation (35)
Total Activation
b = 10.35 cm
Indium Resonance Activation
b = 10.19 cm
10^2
10
8
10
12
14
16
18
r(cm)

Figure 15

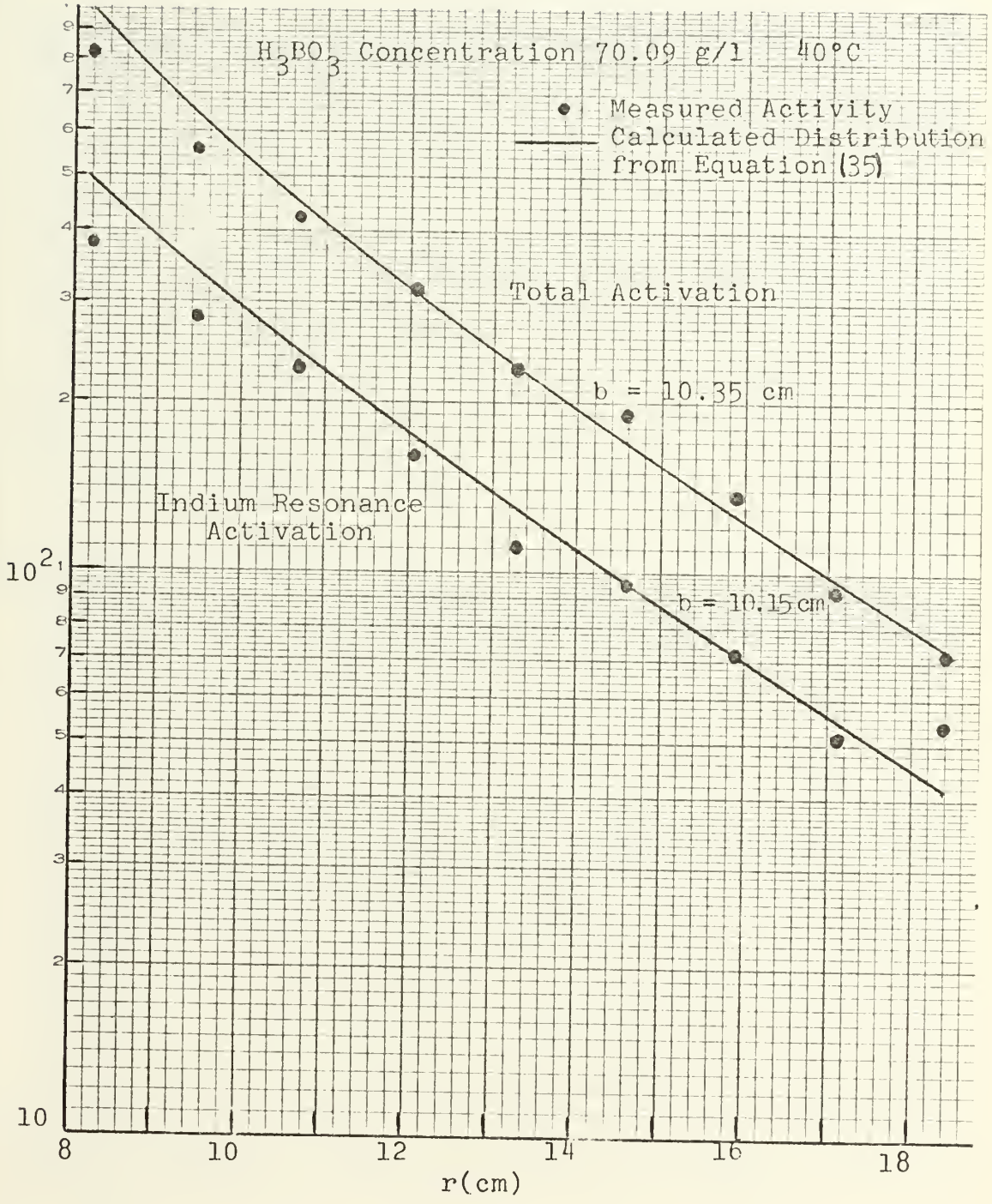
H_3BO_3 Concentration 70.09 g/l 40°C
Measured Activity
Calculated Distribution from Equation (35)
Total Activation
b = 10.35 cm
Indium Resonance Activation
b = 10.15 cm
10^2
10
8
10
12
14
16
18
r(cm)

Figure 16

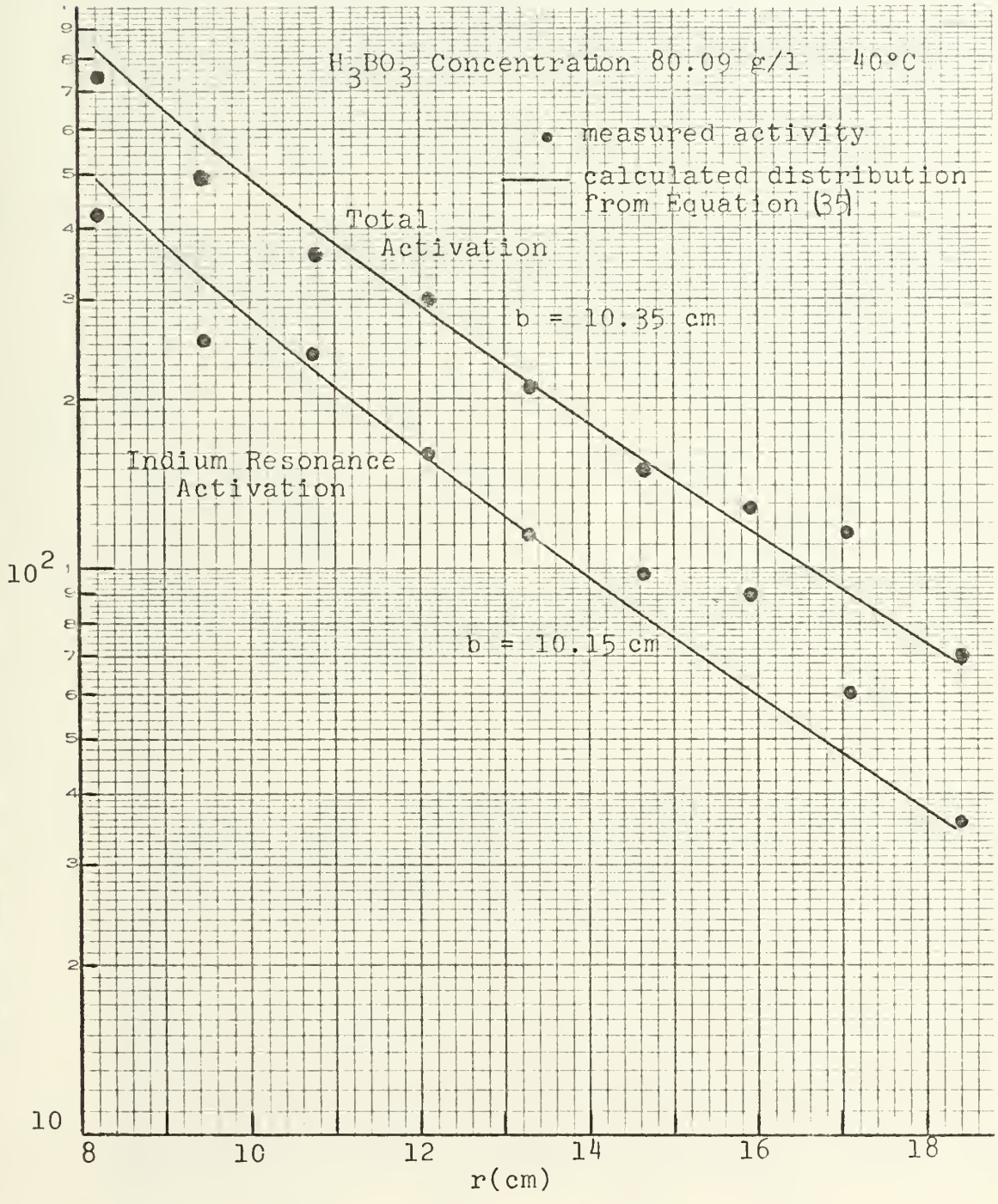
H_3BO_3 Concentration 80.09 g/l 40°C
measured activity
calculated distribution from Equation (35)
Total Activation
b = 10.35 cm
Indium Resonance Activation
b = 10.15 cm
10^2
10
8
10
12
14
16
18
r(cm)

Figure 17

APPENDIX C

PLOTS OF SPHERICAL SPACE DISTRIBUTION,
$A_{CD}r^2$ AND $A_S r^2$, FOR POISON RUNS

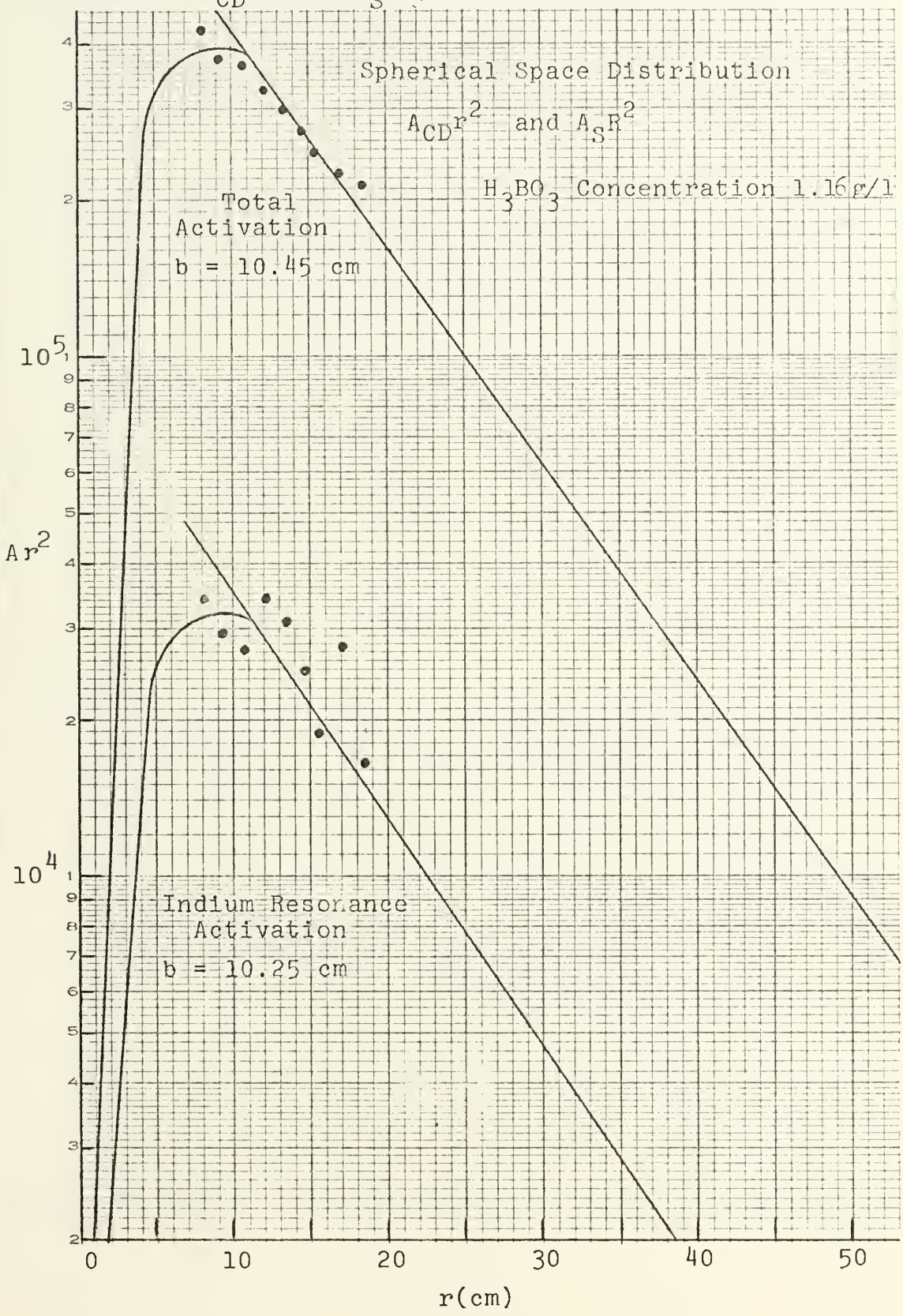

Figure 18

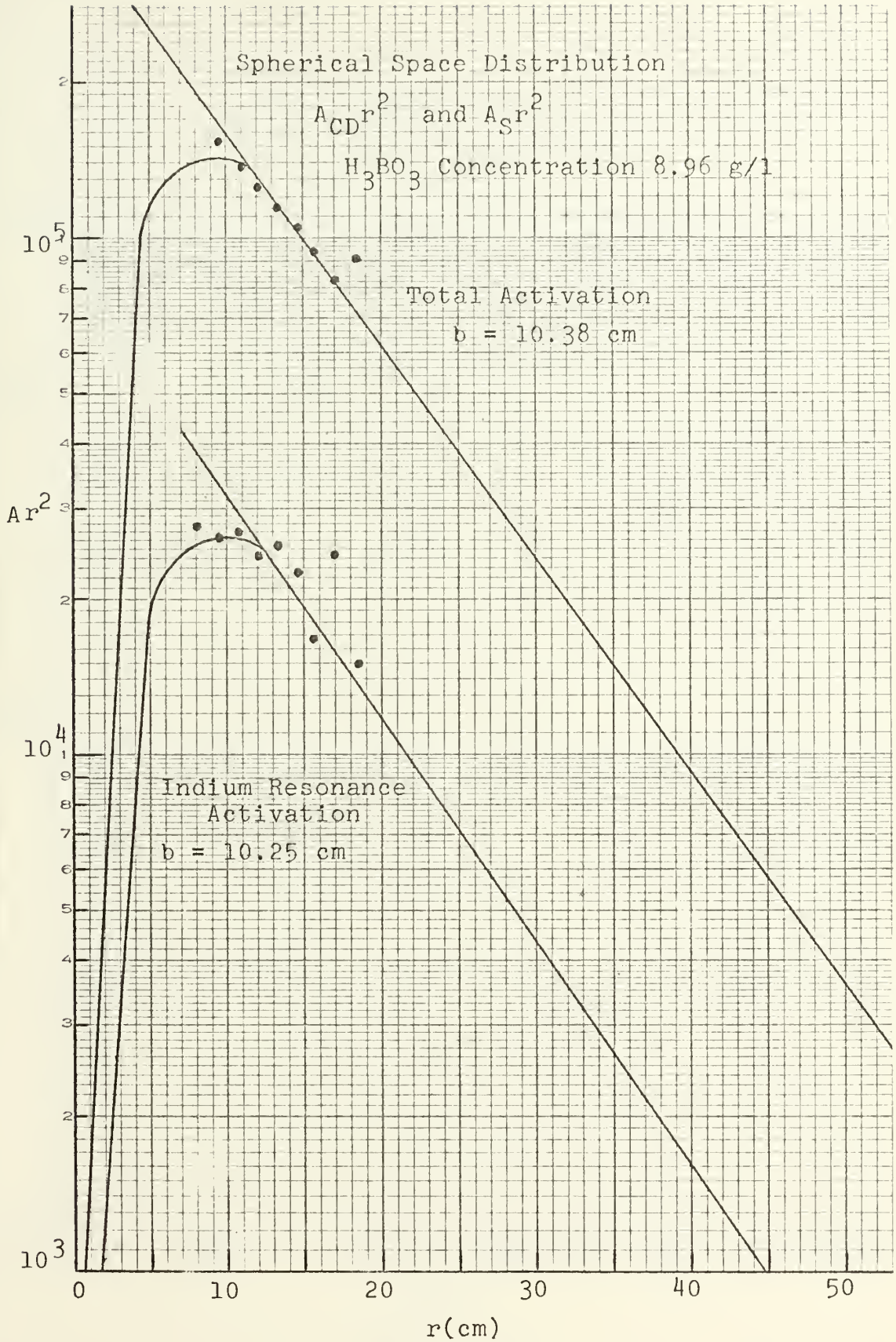
Spherical Space Distribution
$A_{CD}r^2$ and $A_S r^2$
H_3BO_3 Concentration 8.96 g/l
Total Activation
b = 10.38 cm
Indium Resonance
Activation
b = 10.25 cm
Ar^2
10^5
10^4
10^3
0
10
20
30
40
50
r(cm)

Figure 19

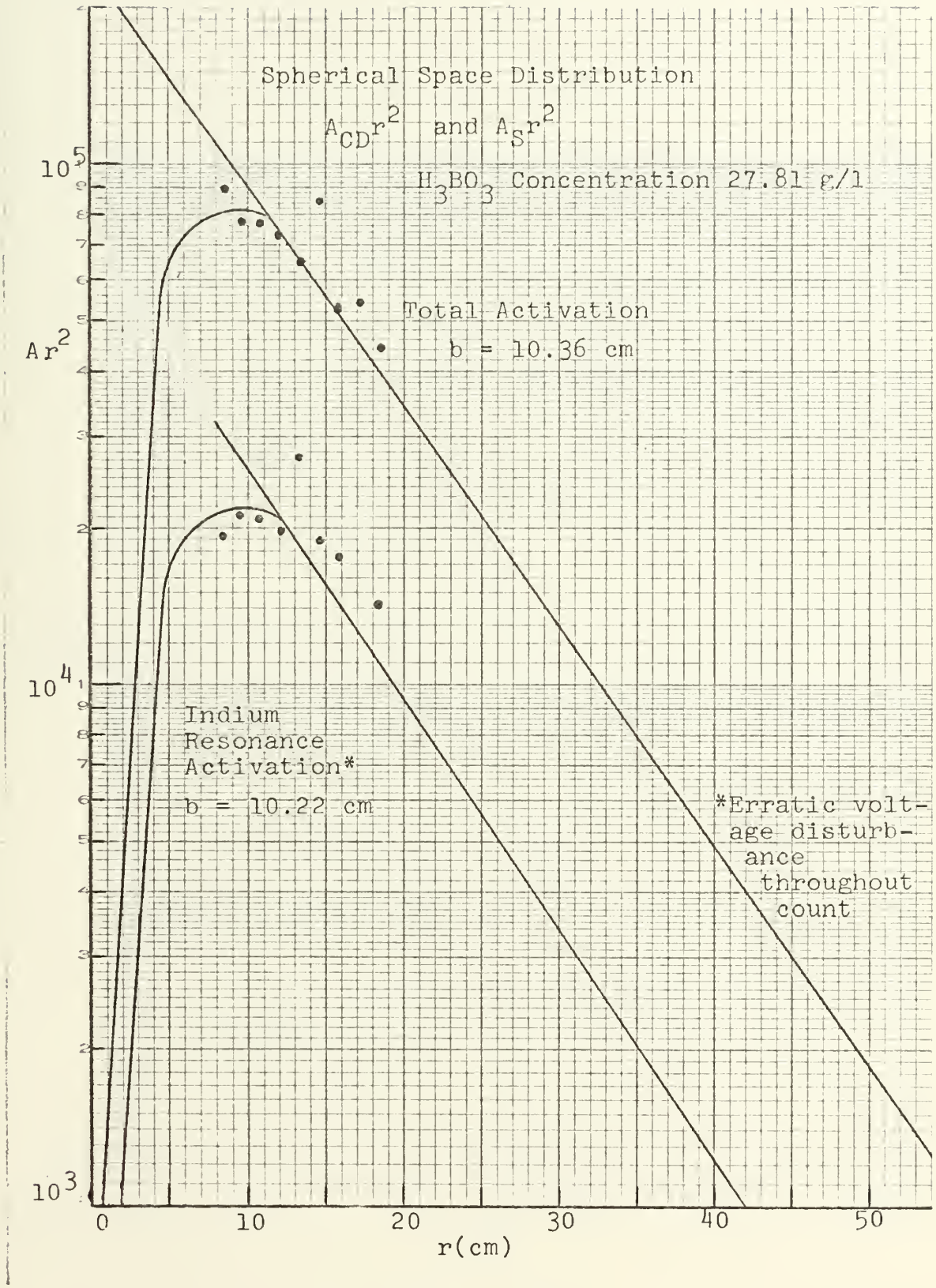
Spherical Space Distribution
$A_{CD}r^2$ and $A_S r^2$
H_3BO_3 Concentration 27.81 g/l
Total Activation
b = 10.36 cm
Indium
Resonance
Activation*
b = 10.22 cm
*Erratic voltage disturbance throughout count
Ar^2
10^5
10^4
10^3
0
10
20
30
40
50
r(cm)

Figure 20

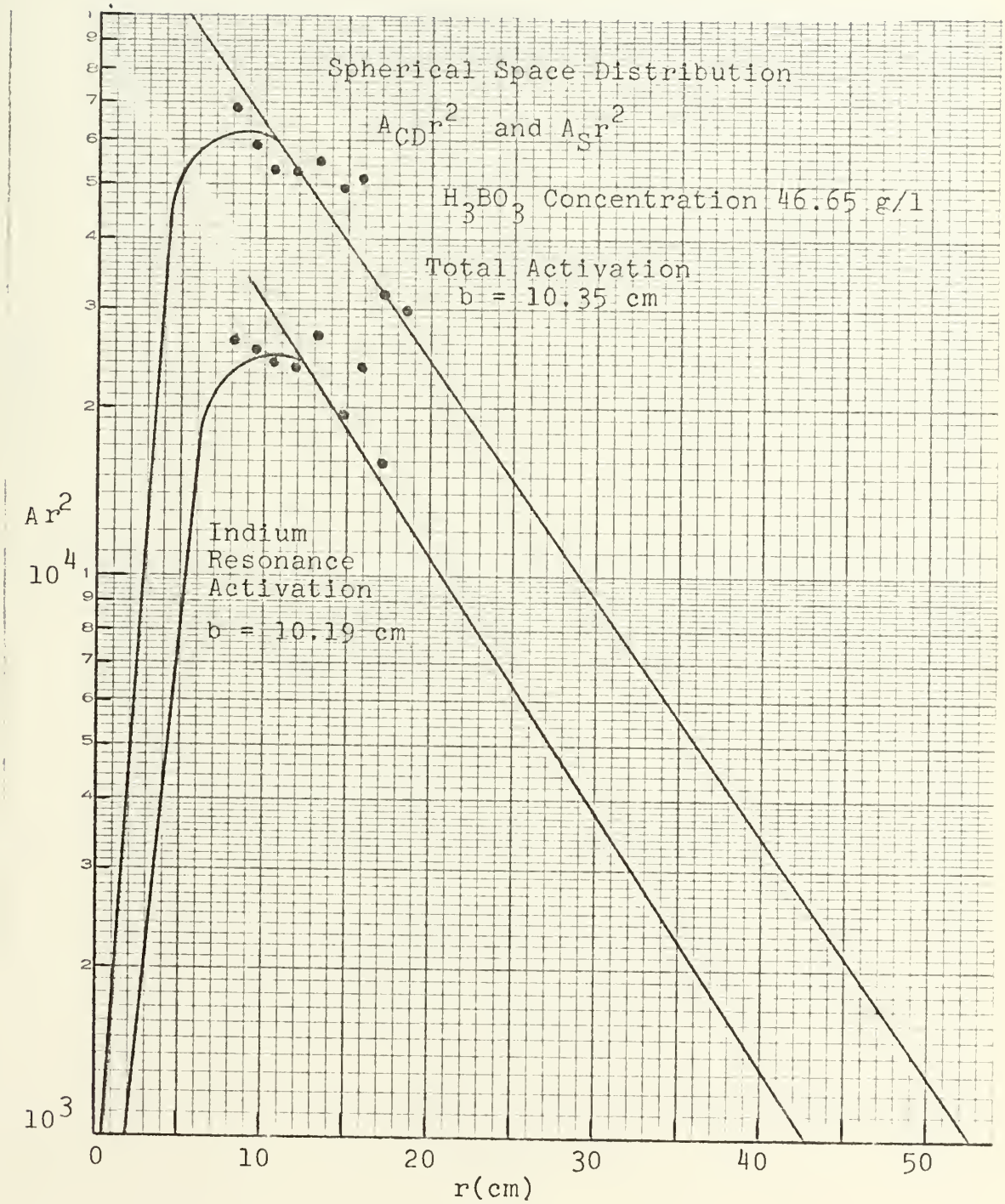
Spherical Space Distribution
$A_{CD}r^2$ and $A_S r^2$
H_3BO_3 Concentration 46.65 g/l
Total Activation
b = 10.35 cm
Indium
Resonance
Activation
b = 10.19 cm
Ar^2
10^4
10^3
0
10
20
30
40
50
r(cm)

Figure 21

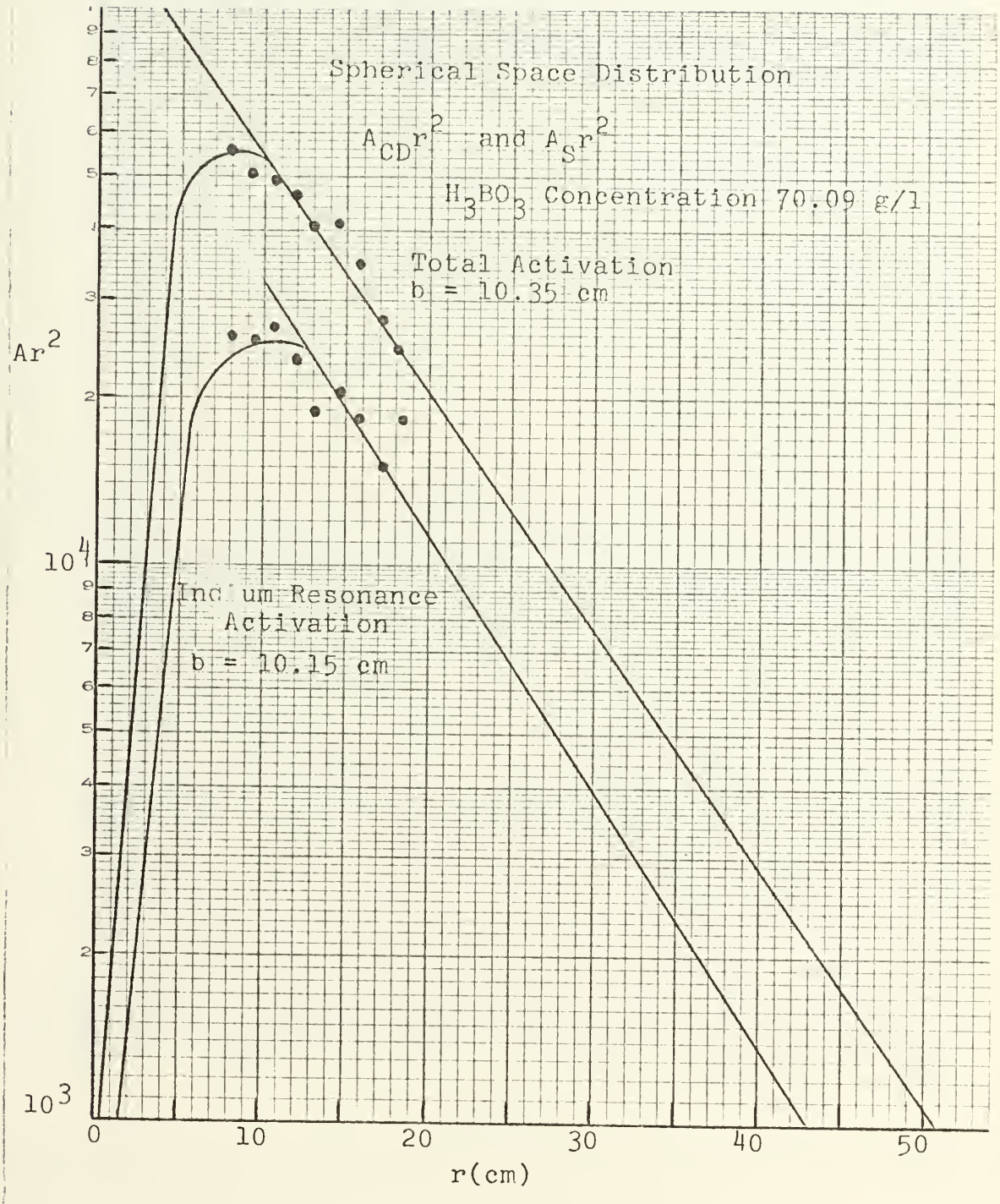
Spherical Space Distribution
$A_{CD}r^2$ and $A_S r^2$
H_3BO_3 Concentration 70.09 g/l
Total Activation
b = 10.35 cm
Indium Resonance
Activation
b = 10.15 cm
Ar^2
10^4
10^3
0
10
20
30
40
50
r(cm)

Figure 22

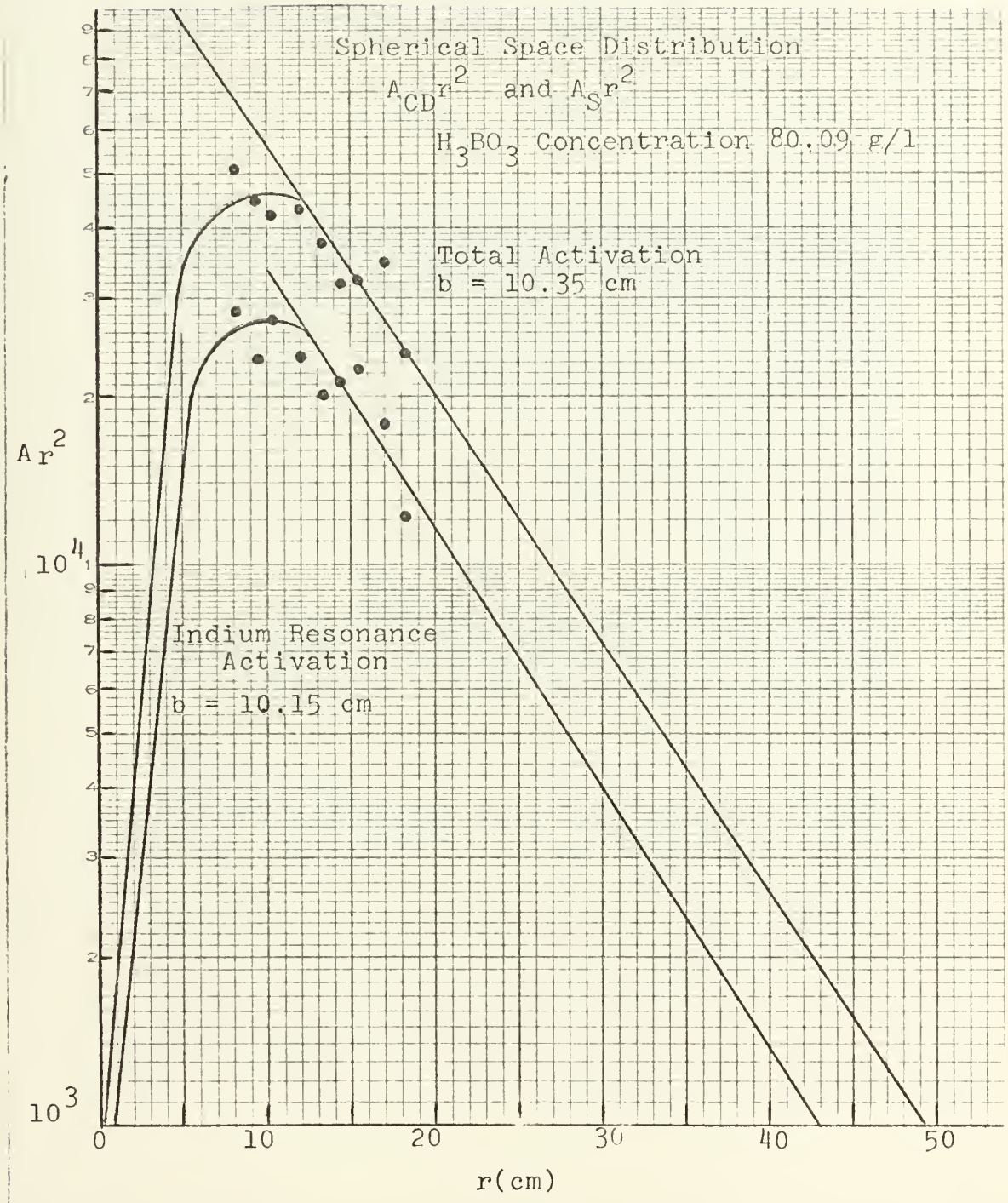
Spherical Space Distribution
$A_{CD}r^2$ and $A_S r^2$
H_3BO_3 Concentration 80.09 g/l
Total Activation
b = 10.35 cm
Indium Resonance
Activation
b = 10.15 cm
Ar^2
10^4
10^3
0
10
20
30
40
50
r(cm)

Figure 23

APPENDIX D

PLOT OF CALCULATED INDIUM RESONANCE ACTIVITY VERSUS r^2 FOR RELAXATION LENGTH OF 10.3 cm

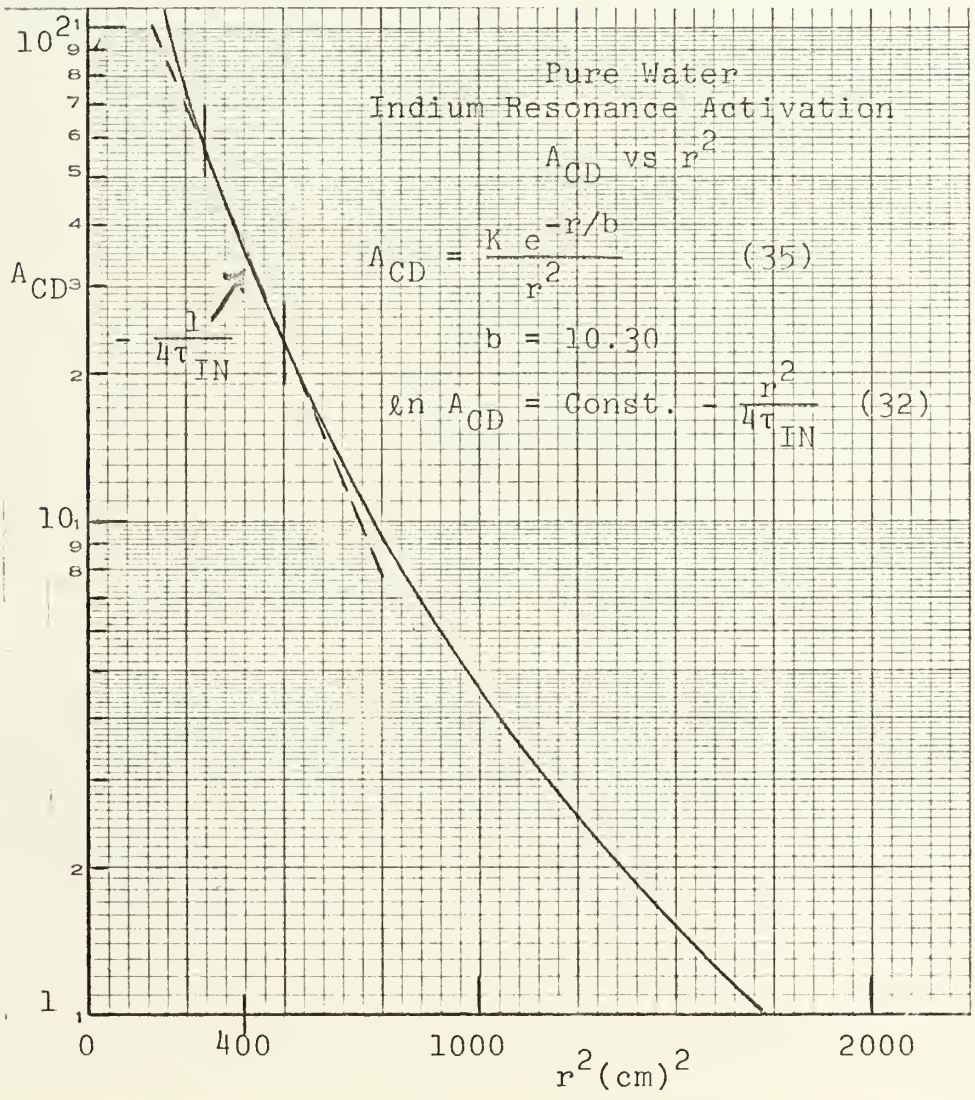

Figure 24

APPENDIX E

PLOTS OF THERMAL FLUX VS r FOR POISON RUNS

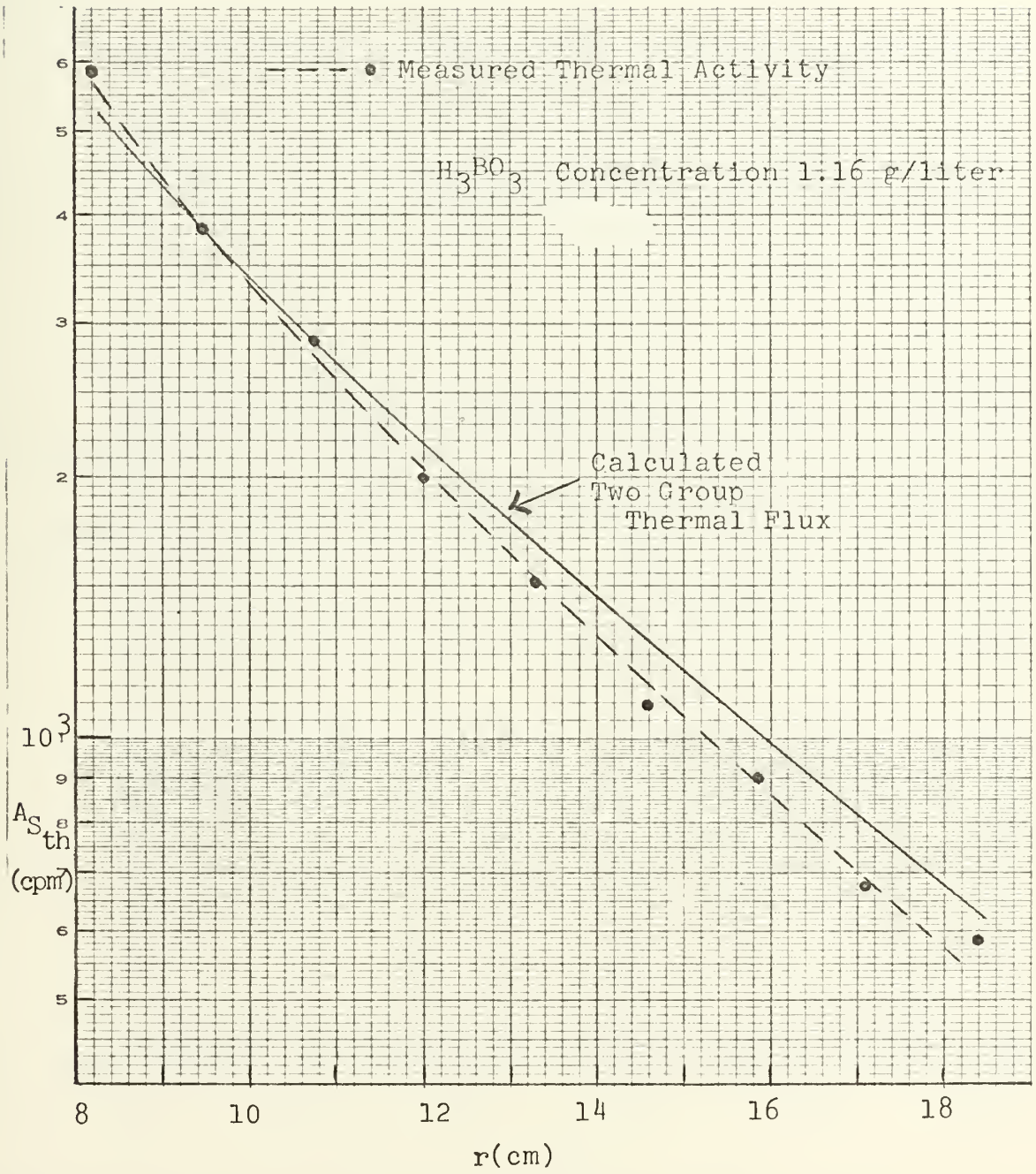

Figure 25

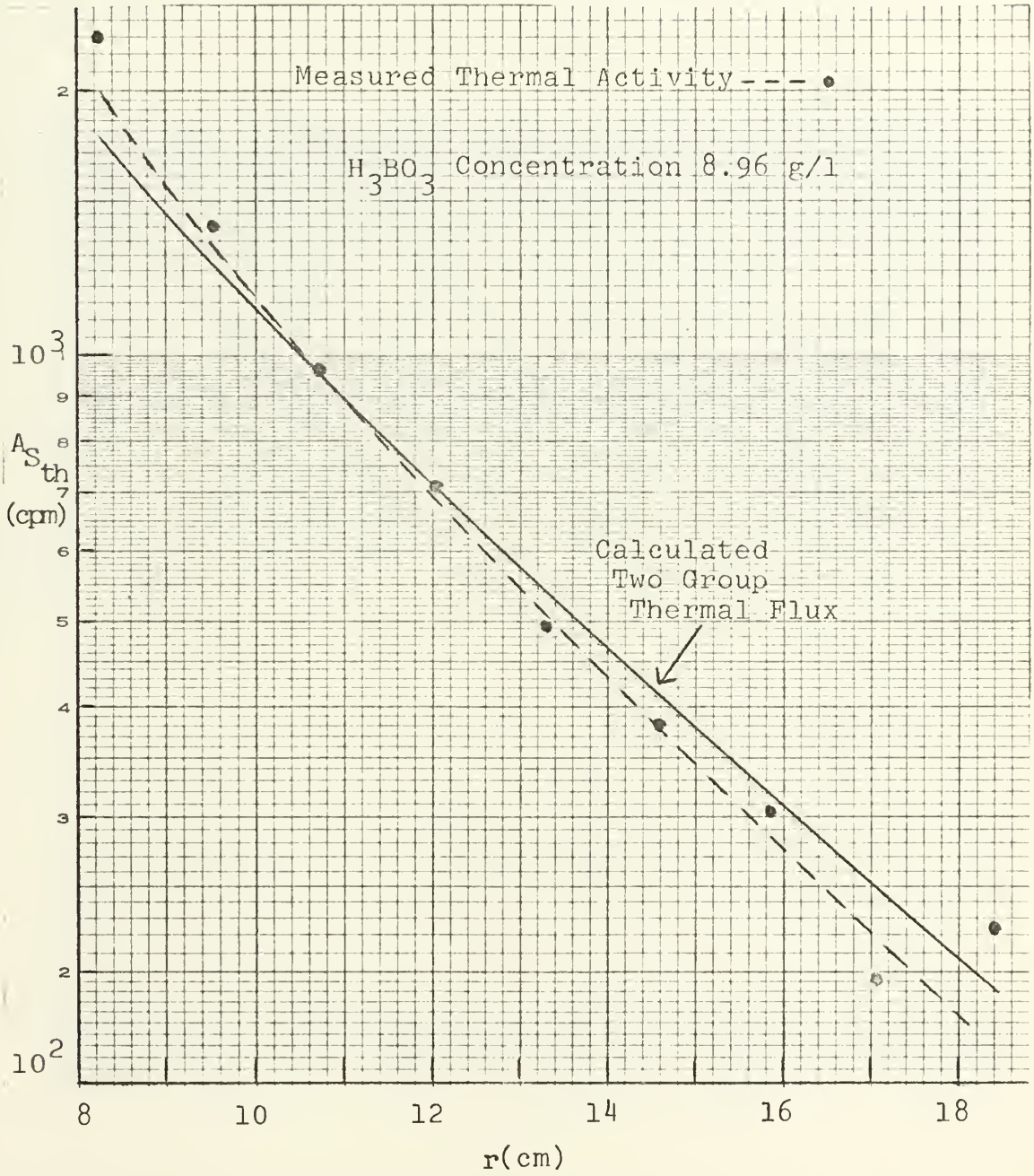
Measured Thermal Activity - - - -
H_3BO_3 Concentration 8.96 g/l
Calculated
Two Group
Thermal Flux
$A_{S_{th}}$
(cpm)
10^3
10^2
2
3
4
5
6
7
8
9
8
10
12
14
16
18
r(cm)

Figure 26

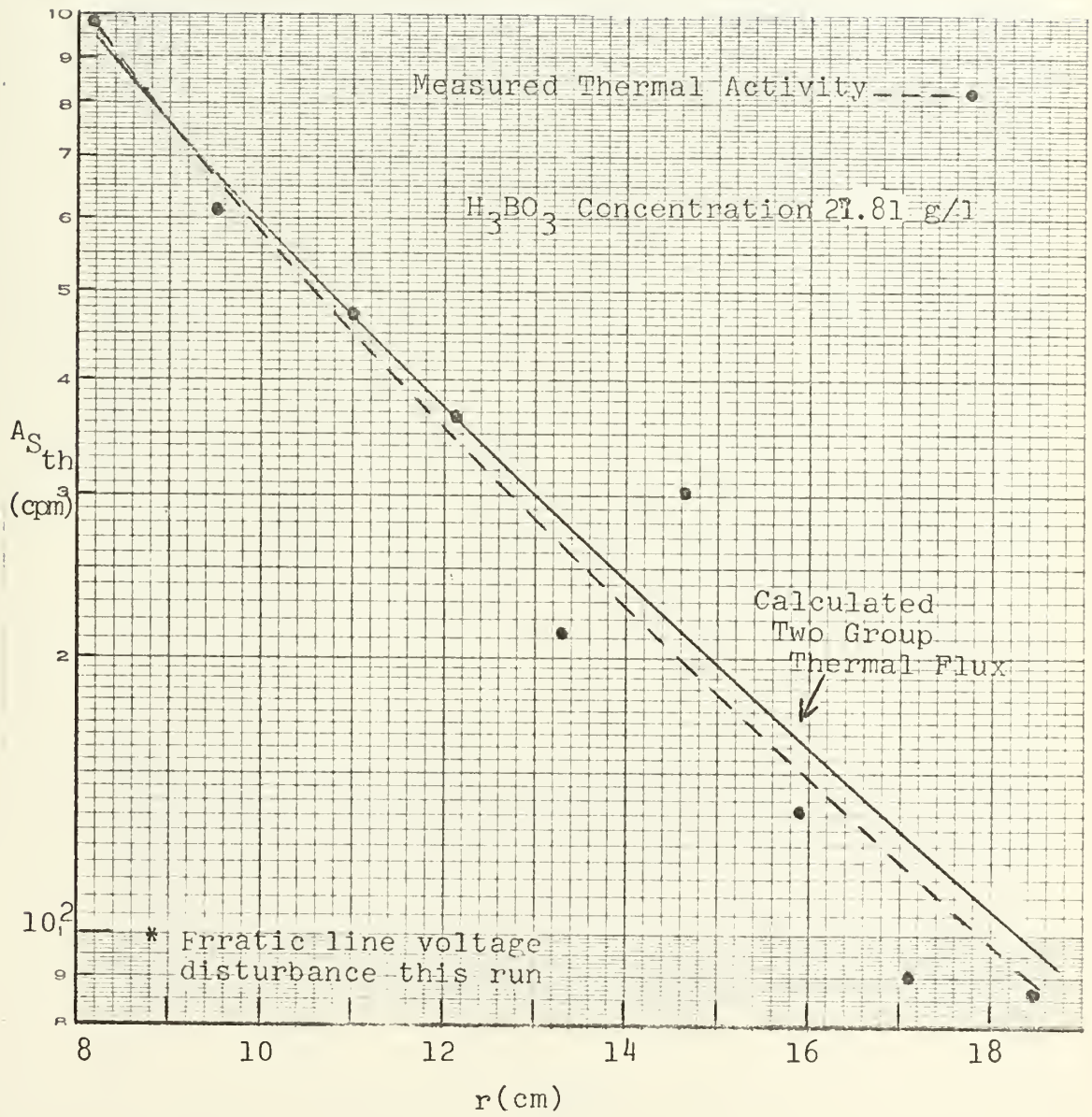
Measured Thermal Activity
H_3BO_3 Concentration 21.81 g/l
Calculated
Two Group
Thermal Flux
* Frratic line voltage
disturbance this run
$A_{S_{th}}$
(cpm)
r(cm)
10
9
8
7
6
5
4
2
10^2
8
10
12
14
16
18

Figure 27

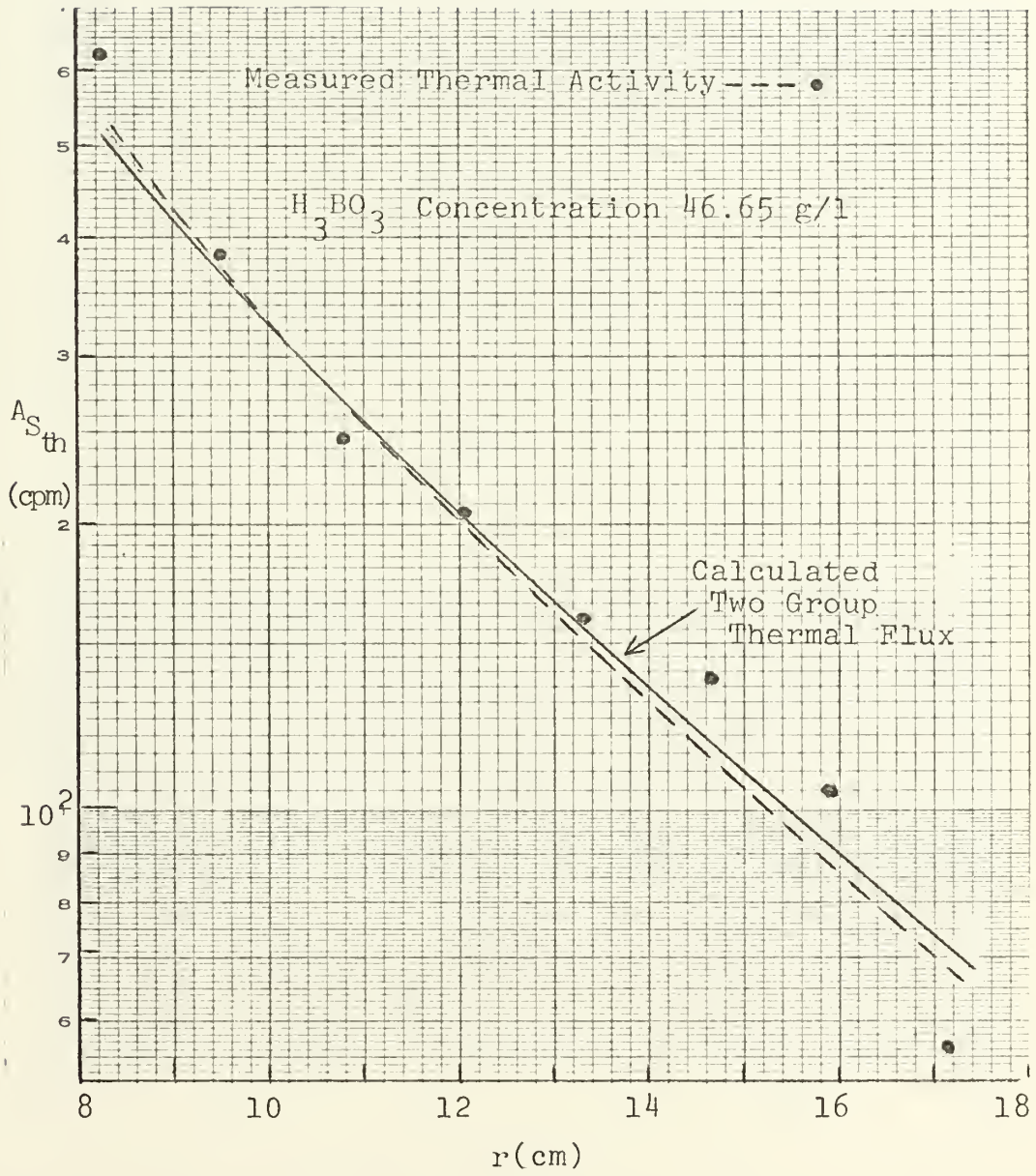
Measured Thermal Activity - - -
H_3BO_3 Concentration 46.65 g/l
$A_{S_{th}}$
(cpm)
Calculated
Two Group
Thermal Flux
10^2
6
5
4
3
2
9
8
7
6
8
10
12
14
16
18
r(cm)

Figure 28

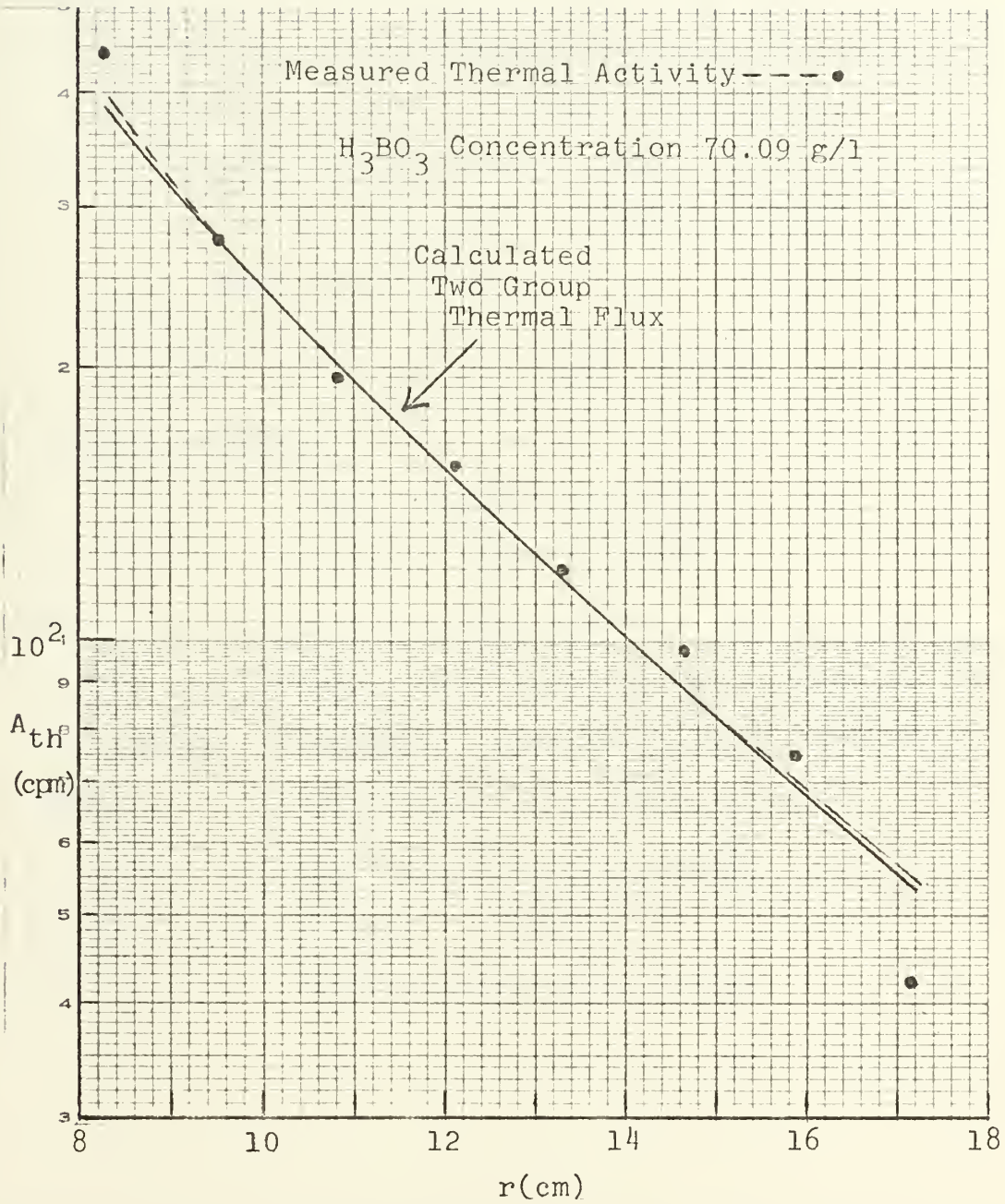
Measured Thermal Activity
H_3BO_3 Concentration 70.09 g/l
Calculated
Two Group
Thermal Flux
10^2
A_{th}
(cpm)
8
10
12
14
16
18
r(cm)

Figure 29

APPENDIX F

COMPUTER PROGRAM 1

A. PURPOSE

1. To correct counting data and compute the saturated activity in counts per minute (A_{CD} and A_S).
2. To compute the approximate mean counting rate and, from this, determine the standard deviation based on a normal distribution.
3. To compute the products $A_{CD}r^2$ and A_Sr^2.

B. PROGRAM NOTATION

D	Decay constant for IN^{116}
T	Counter resolving time
POS	Distance from source
C, CC	Ten minute counts (side 1, side 2)
ASAT, BSAT	Saturated activity (side 1, side 2)
AMEAN	Approximate mean counting rate
W	Correction for foil weight
SIGMA	Standard deviation
F	Cadmium correction factor

APPENDIX F

COMPUTER PROGRAM 1

```
      IMPLICIT REAL*8(A-H,O-Z)
      WRITE(6,1)
    1 FORMAT(T5,'DISTANCE',T25,'SAT ACTIVITY',T56,'MEAN',
     1T87,'SIGMA'//)
      D=1.28D-2
      T=6.CD-6
      DO500 M=1,2
      DO50 N=1,9
      READ(5,2) POS,C,X,Y,Z,CC,YY,ZZ
    2 FORMAT(8F9.0)
      READ(5,6) W
    6 FORMAT(1F9.0)
      DIST=POS*0.254D01
      C=W*C/(1.CDO-C*T)
      CC=W*CC/(1.0DO-CC*T)
      ASAT=D*C/((1.0DO-DEXP(-D*X))*(DEXP(-D*Y)-DEXP(-D*Z)))
      BSAT=D*CC/((1.0DO-DEXP(-D*X))*(DEXP(-D*YY)-DEXP(-D*ZZ)
     1))
      SAT=(ASAT+BSAT)/2.0DO
      AMEAN=(C+CC)/2.0D01
      SIGMA=AMEAN**0.5DO
      F=1.11DO
      FSAT=F*SAT
      WRITE(6,4) DIST,FSAT,AMEAN,SIGMA
    4 FORMAT(T6,F5.2,6X,D25.16,6X,D25.16,6X,D25.16)
      A=FSAT*DIST**2.0DO
      B=FSAT*DIST**4.0DO
    8 FORMAT(/,T12,F5.2,6X,D25.16,6X,D25.16)
      WRITE(6,8) DIST,A,B
   50 CONTINUE
      DO60 N=1,9
      READ(5,5) POS,C,X,Y,Z,CC,YY,ZZ
    5 FORMAT(8F9.0)
      READ(5,7) W
    7 FORMAT(1F9.0)
      DIST=POS*0.254D01
      C=W*C/(1.0DO-C*T)
      CC=W*CC/(1.0DO-CC*T)
      ASAT=D*C/((1.0DO-DEXP(-D*X))*(DEXP(-D*Y)-DEXP(-D*Z)))
      BSAT=D*CC/((1.0DO-DEXP(-D*X))*(DEXP(-D*YY)-DEXP(-D*ZZ)
     1))
      SAT=(ASAT+BSAT)/2.0DO
      AMEAN=(C+CC)/2.0D01
      SIGMA=AMEAN**0.5DO
      WRITE(6,3) DIST,SAT,AMEAN,SIGMA
    3 FORMAT(T6,F5.2,6X,D25.16,6X,D25.16,6X,D25.16)
      A=SAT*DIST**2.0DO
      B=SAT*DIST**4.0DO
      WRITE(6,9) DIST,A,B
    9 FORMAT(/,T12,F5.2,6X,D25.16,6X,D25.16)
   60 CONTINUE
  500 CONTINUE
      STOP
      END
```

APPENDIX G

COMPUTER PROGRAM 2

A. PURPOSE

1. To compute the area under curved portions of the curves $A_{CD}r^2$, $A_S r^2$, $A_{CD}r^4$ and $A_S r^4$ versus r using Simpson's Rule.
2. To compute area under straight line portions of these curves analytically.
3. To compute total areas and, from this, M_T^2 and τ_{IN} using Equations (13) and (18).
4. To compute τ_T by correcting τ_{IN} for additional age required to reach thermal energies.
5. To compute diffusion length by solving

$$L_T = (M_T^2 - \tau_T)^{\frac{1}{2}}$$

B. PROGRAM NOTATION

y(I)	Ordinate values of $A_{CD}r^2$, $A_S r^2$, $A_{CD}r^4$ and $A_S r^4$
H	Abscissa interval lengths in cm. used to obtain y(I) values.
N	Number of abscissa intervals, H.
S(J)	Simpson area approximations
B(I)	Relaxation Length values
Z(I)	Ordinate values of $A_{CD}r^2$, $A_S r^2$, $A_{CD}r^4$ and $A_S r^4$ corresponding to abscissa values of r at which distributions become exponential.

A(I)	Area under exponential portion of curves.
AA(I)	Total area under curves. AA(I) = S(J) + A(I).
MIG(I)	Thermal Migration area values.
AGE(I)	Values of neutron age to Indium Resonance.
Y(I)	Diffusion Lengths.

APPENDIX G

COMPUTER PROGRAM 2

```
COMPUTING SATURATED ACTIVITY TIMES DISTANCE SQUARED AREAS
      IMPLICIT REAL*8(A-H,O-Z)
      REAL*8MIG
      DIMENSION Y(80),S(28),B(28),Z(28),A(28),AA(28),
     1MIG(28),AGE(28)
      DO80 J=1,14
      READ(5,10) (Y(I),I=1,11)
   10 FORMAT(1F10.0)
      H=1.25
      N=10
      SUM2=0.0DO
      DO5O L=2,N,2
   5O SUM2= SUM2+Y(L)
      SUM3=0.0DO
      M=N-1
      DO6O K=3,M,2
   6O SUM3=SUM3+Y(K)
      S(J)=H/0.3D1*(Y(1)+0.4D1*SUM2+0.2D1*SUM3+Y(N+1))
      WRITE(6,7O) S(J)
   7O FORMAT(T19,'SIMPSON APPROXIMATION=',D25.16///)
   8O CONTINUE
COMPUTING ACTIVITY TIMES DISTANCE TO THE FOURTH AREAS
      DO9O J=15,28
      READ(5,11) (Y(I),I=1,19)
   11 FORMAT(1F10.0)
      H=2.5DO
      N=18
      SUM2=0.0DO
      DO51 L=2,N,2
   51 SUM2=SUM2+Y(L)
      SUM3=0.0DO
      M=N-1
      DO61 K=3,M,2
   61 SUM3=SUM3+Y(K)
      S(J)=H/O.3D1*(Y(1)+0.4D1*SUM2+0.2D1*SUM3+Y(N+1))
      WRITE(6,71) S(J)
   71 FORMAT(T19,'SIMPSON',D25.16///)
   9O CONTINUE
COMPUTING AREAS UNDER LINEAR PORTION OF CURVES
      READ(5,1) (B(I),Z(I),I=1,28)
    1 FORMAT(2F1O.0)
      DO2 I=1,28
      A(I)=Z(I)/B(I)
      WRITE(6,3) B(I),A(I)
    3 FORMAT(2E14.7///)
    2 CONTINUE
      DO100 I=1,28
  100 AA(I)=A(I)+S(I)
      DO200 I=1,13,2
      MIG(I)=AA(I+14)/(AA(I)*6.0)
      WRITE(6,201) MIG(I)
  201 FORMAT(T19,'MIGRATION AREA=',D25.16///)
  20O CONTINUE
      DO300 I=2,14,2
      AGE(I)=AA(I+14)/(AA(I)*6.0)
      WRITE(6,301) AGE(I)
  301 FORMAT(T19,'AGE=',D25.16///)
  30O CONTINUE
      DO400 I=2,14,2
      Y(I)=(MIG(I-1)-(AGE(I)+1.8))**0.5
      WRITE(6,401) Y(I)
  401 FORMAT(T19,'DIFFUSION LENGTH=',D25.16//)
  40O CONTINUE
      STOP
      END
```

APPENDIX H

COMPUTER PROGRAM 3

A. PURPOSE

1. To determine slope of curve $\ell n A_{th}$ vs. r^2 in the range $18.4 \leq r \leq 22$ cm. by the method of least squares.

2. To compute τ_{IN} from the relation

$$\text{slope} = -\frac{1}{4\tau_{IN}}$$

B. PROGRAM NOTATION

F(I) Relaxation length values

G(I) Values of neutron age and thermal migration area

X(I) Distances from the source

Z(J) Solutions to equation

$$Z = \frac{Ce^{-r/b}}{r^2}$$

Y(I) Natural logarithm of Z values
$Y = \ell n\ Z = a_1 + a_2 x$

SIMQ Subroutine for solving system of equations $CA = B$:

$$\underset{C}{\begin{bmatrix} 7 & \sum_{i=1}^{7} x_i \\ \sum_{i=1}^{7} x_i & \sum_{i=1}^{7} x_i^2 \end{bmatrix}} \underset{A}{\begin{bmatrix} a_1 \\ a_2 \end{bmatrix}} = \underset{B}{\begin{bmatrix} \sum_{i=1}^{7} y_i \\ \sum_{i=1}^{7} x_i y_i \end{bmatrix}}$$

a_2 Slope of straight line solution equal to the negative reciprocal of $4\tau_{IN}$

APPENDIX H

COMPUTER PROGRAM 3

```
      DIMENSION X(9),Y(9),Z(9),XC(2),C(2,2),
     1B(2),A(2),D(7),F(7),G(9)
      READ(5,5) (D(I),F(I),I=1,6)
    5 FORMAT(2F9.0)
      READ(5,56) (G(I),I=1,6)
   56 FORMAT(F9.0)
      DO6 L=1,6
      X(1)=18.41
      X(2)=18.7
      X(3)=19.2
      X(4)=19.5
      X(5)=19.7
      X(6)=20.0
      X(7)=22.0
      DO9 J=1,7
      Z(J)=(D(L)*EXP(-X(J)/F(L)))/X(J)**2.0
    9 CONTINUE
      DO11 I=1,7
   11 Y(I)=ALOG(Z(I))
      DO12 I=1,7
   12 X(I)=X(I)**2.0
SUMMING POWERS OF X(I)
      DO 20 K=1,2
      XC(K)=0.0
      DO15 I=1,7
   15 XC(K)=XC(K)+X(I)**K
   20 CONTINUE
SUMMING Y(I)
      YC=0.0
      DO22 I=1,7
   22 YC=YC+Y(I)
      YX=0.0
      DO25 I=1,7
   25 YX=YX+Y(I)*X(I)
FORMING TWO EQUATIONS CA=B WITH ELEMENTS IN COLUMNS
      DO40 I=1,2
      DO35 J=1,2
      JUG1=I+J-2
      IF(JUG1)33,33,31
   33 C(1,1)=7.0
      GOTO 35
   31 C(I,J)=XC(JUG1)
   35 CONTINUE
   40 CONTINUE
      B(1)=YC
      B(2)=YX
      CALL SIMQ(C,B,2,KS)
      WRITE(6,50) KS
   50 FORMAT(T5,'ERROR=',I3)
      DO52 I=1,2
   52 A(I)=B(I)
      WRITE(6,54) A(1),A(2)
   54 FORMAT(T5,'A(1)=',E14.7/T5,'A(2)=',E14.7)
      AGE=0.29/A(2)
      WRITE(6,55) AGE
   55 FORMAT(T15,'AGE=',E14.7//)
    6 CONTINUE
      STOP
      END
```

APPENDIX I

RESULTS OF COMPUTER PROGRAM 1

TABLE 8

PURE WATER; INDIUM RESONANCE ACTIVATION

r(cm)	A_{CD}(CPM)	Mean Count	Standard Deviation
8.26	298.0691	233.2133	15.2713
9.52	204.1689	157.3879	12.5454
10.79	155.0969	118.2727	10.8753
12.07	124.0281	89.9505	9.4842
13.34	78.4197	19.3193	4.3954
14.61	67.7517	50.4245	7.1010
15.88	50.9003	39.3977	6.2767
17.14	42.2404	32.7216	5.7203
18.41	34.2155	25.6226	5.0618

TABLE 9

PURE WATER; TOTAL ACTIVATION

r(cm)	A_S(CPM)	Mean Count	Standard Deviation
8.26	4459.2573	3663.2972	60.5252
9.52	3549.0267	2918.2418	54.0207
10.79	2747.3121	2259.8505	47.5378
12.07	1930.5774	1664.8222	40.8022
13.34	1437.4071	1181.5408	34.3735
14.61	1090.0382	900.1418	30.0023
15.88	852.3489	692.3284	26.3121
17.14	642.0987	529.1137	23.0024
18.41	541.2537	449.0388	21.1905

TABLE 10

H_3BO_3 CONCENTRATION 1.16 g/l; INDIUM RESONANCE ACTIVATION

r(cm)	A_{CD}(CPM)	Mean Count	Standard Deviation
8.26	503.1124	379.3378	19.4766
9.52	322.7215	240.9674	15.5231
10.79	233.0711	176.0013	13.2665
12.07	233.6401	175.2742	13.2391
13.34	172.9660	129.3376	11.3726
14.61	116.5811	90.3156	9.5035
15.88	74.4533	57.2474	7.5662
17.14	94.6393	72.5835	8.5196
18.41	48.3223	36.5259	6.0436

TABLE 11

H_3BO_3 CONCENTRATION 1.16 g/l; TOTAL ACTIVATION

r(cm)	A_S(CPM)	Mean Count	Standard Deviation
8.26	6261.3213	5172.9621	71.9233
9.52	4148.3711	3446.4026	58.7061
10.79	3113.6634	2596.8206	50.9590
12.07	2229.4831	1854.0849	43.0591
13.34	1681.5223	1400.5575	37.4240
14.61	1265.8901	1080.4300	32.8698
15.88	986.9352	842.4719	29.0254
17.14	768.5511	639.9204	25.2966
18.41	635.0632	527.7004	22.9717

TABLE 12

H_3BO_3 CONCENTRATION 8.96 g/l; INDIUM RESONANCE ACTIVATION

r(cm)	A_{CD}(CPM)	Mean Count	Standard Deviation
8.26	409.9467	314.5537	17.7356
9.52	291.4477	213.2623	14.6035
10.79	229.5099	167.0131	12.9233
12.07	167.2182	123.1536	11.0975
13.34	142.2078	103.2886	10.1631
14.61	105.7302	81.3866	9.0215
15.88	67.2199	51.4156	7.1705
17.14	83.3672	62.9565	7.9345
18.41	44.4031	33.5245	5.7900

TABLE 13

H_3BO_3 CONCENTRATION 8.96 g/l; TOTAL ACTIVATION

r(cm)	A_S(CPM)	Mean Count	Standard Deviation
8.26	2713.8679	2326.7305	48.2361
9.52	1704.0191	1413.4715	37.5961
10.79	1188.5005	986.2288	31.4042
12.07	871.8115	725.4009	26.9333
13.34	639.1190	530.0796	23.0235
14.61	487.743	405.6754	20.1414
15.88	373.6443	310.4774	17.6204
17.14	279.7307	226.8509	15.0616
18.41	269.3002	220.0322	14.8334

TABLE 14

H_3BO_3 CONCENTRATION 27.81 g/l; INDIUM RESONANCE ACTIVATION

r(cm)	A_{CD}(CPM)	Mean Count	Standard Deviation
8.26	285.2747	218.7960	14.7918
9.52	236.3981	183.6949	13.5534
10.79	179.0414	138.1119	11.7521
12.07	135.2377	103.4736	10.1722
13.34	146.9174	107.5823	10.3722
14.61	89.3376	66.5402	8.5721
15.88	69.3343	51.0123	7.1423
17.14	93.9194	73.3271	8.5631
18.41	42.0807	32.5463	5.7049

TABLE 15

H_3BO_3 CONCENTRATION 27.81 g/l; TOTAL ACTIVATION

r(cm)	A_S(CPM)	Mean Count	Standard Deviation
8.26	1313.3395	1118.5688	33.4450
9.52	855.6882	729.7254	27.0134
10.79	658.1651	558.1721	23.6256
12.07	503.8277	427.9465	20.6868
13.34	360.5809	306.2933	17.5012
14.61	399.0305	332.2687	18.2282
15.88	206.7903	176.8829	13.2997
17.14	186.5858	158.2384	12.5793
18.41	129.9547	110.3157	10.5031

TABLE 16

H_3BO_3 CONCENTRATION 46.65 g/l; INDIUM RESONANCE ACTIVATION

r(cm)	A_{CD}(CPM)	Mean Count	Standard Deviation
8.26	383.1435	297.7103	17.2543
9.52	282.4397	212.2461	14.5761
10.79	207.4628	153.5804	12.3927
12.07	162.0674	119.9549	10.9524
13.34	150.3377	113.8245	10.6688
14.61	90.8321	67.9496	8.2432
15.88	95.1983	71.8575	8.4768
17.14	54.4682	40.6000	6.3718
18.41	79.3777	57.6782	7.5946

TABLE 17

H_3BO_3 CONCENTRATION 46.65 g/l; TOTAL ACTIVATION

r(cm)	A_S(CPM)	Mean Count	Standard Deviation
8.26	1006.1537	835.3732	28.9028
9.52	652.8737	542.5276	23.2922
10.79	455.5653	377.8619	19.4387
12.07	364.3542	304.2721	17.4434
13.34	310.0154	251.2099	15.8496
14.61	229.8385	186.2102	13.6458
15.88	199.8872	159.1900	12.6172
17.14	110.6291	91.8081	9.5816
18.41	88.0501	73.0562	8.5473

TABLE 18

H_3BO_3 CONCENTRATION 70.09 g/l; INDIUM RESONANCE ACTIVATION

r(cm)	A_{CD}(CPM)	Mean Count	Standard Deviation
8.26	379.0630	285.6253	16.9004
9.52	282.1943	214.0142	14.6292
10.79	230.4439	165.9322	12.8814
12.07	160.5295	120.9588	10.9981
13.34	106.3356	79.5638	8.9198
14.61	95.0191	69.8891	8.3599
15.88	72.4740	55.6762	7.4617
17.14	51.1528	38.2288	6.1829
18.41	54.6934	41.7976	6.4651

TABLE 19

H_3BO_3 CONCENTRATION 70.09 g/l; TOTAL ACTIVATION

r(cm)	A_S(CPM)	Mean Count	Standard Deviation
8.26	824.4368	683.2489	26.1391
9.52	558.2886	462.7575	21.5117
10.79	426.2032	354.2170	18.8206
12.07	316.5702	261.6614	16.1759
13.34	228.9763	189.6963	13.7730
14.61	192.6427	159.1687	12.6162
15.88	137.7566	114.1718	10.6851
17.14	93.6648	79.3185	8.9061
18.41	72.2664	60.5687	7.7826

TABLE 20

H_3BO_3 CONCENTRATION 80.09 g/l; INDIUM RESONANCE ACTIVATION

r(cm)	A_{CD}(CPM)	Mean Count	Standard Deviation
8.26	414.8513	307.2195	17.5277
9.52	256.6541	196.2806	14.0100
10.79	239.3121	177.5645	13.3253
12.07	161.0497	122.6576	11.0751
13.34	113.0485	87.4346	9.3506
14.61	99.8647	77.9423	8.8285
15.88	90.3185	68.9324	8.3026
17.14	60.4457	45.0622	6.7128
18.41	35.4877	27.8769	5.2799

TABLE 21

H_3BO_3 CONCENTRATION 80.09 g/l; TOTAL ACTIVATION

r(cm)	A_S(CPM)	Mean Count	Standard Deviation
8.26	743.8847	614.4305	24.7877
9.52	494.7427	419.9927	20.4937
10.79	360.5303	309.5135	17.5929
12.07	302.0725	261.4078	16.1681
13.34	212.3189	175.3501	13.2419
14.61	149.1620	128.0910	11.3177
15.88	127.8776	105.3823	10.2656
17.14	116.5993	99.1096	9.9554
18.41	70.7709	53.4546	7.3113

BIBLIOGRAPHY

1. Corngold, N., Nuclear Science and Engineering, 19, 80 (1964).

2. Williams, M. M. R., The Slowing Down and Thermalization of Neutrons, North-Holland Publishing Company, 1966.

3. Goddard, A. J. H. and Johnson, P. W., Nuclear Science and Engineering, 37, 127 (1969).

4. Starr, E. and Koppel, J., Nuclear Science and Engineering, 6, 162 (1959).

5. Reier, M. and Dejuren, J., WAPD-MTJ-8, (1959)

6. Glasstone, S. and Edlund, M. C., The Elements of Nuclear Reactor Theory, D. Van Nostrand Company, Inc., (1952).

7. Hess, W. H., Annals of Physics: 2, 115 (1959).

8. Jakeman, D., Physics of Nuclear Reactors, American Elsevier Publishing Company, 1966.

9. Larmarsh, J. R., Introduction to Nuclear Reactor Theory. Addison-Wesley, 1966.

10. Meghreblian, R. V. and Holmes, D. K. Reactor Analysis, McGraw Hill Book Company, 1960.

11. Valente, F. A., A Manual of Experiments in Reactor Physics, Macmillan Company, 1963.

12. PU-BE Source Experimental Manual, Reactor Experiments, Inc.

13. Price, W. J., Nuclear Radiation Detection, McGraw-Hill Book Company, 1964.

14. Tittle, C. W., Nucleonics, 9, 60 (1951).

15. Foster, D. G., Nuclear Science and Engineering, 8, 148 (1960).

16. Rush, J. H., Physical Review, 73, 271 (1948).

17. ANL-5800, Reactor Physics Constants, United States Energy Commission, 1963.

18. Wilkins, J. E., Hellens, R. L., Zweifel, P. E., Proceedings of International Conference on Peaceful Uses of Atomic Energy, 5, 62 (1956).

19. Valente, F. A., Sullivan, R. E., Nuclear Science and Engineering, 6, 162 (1959).

INITIAL DISTRIBUTION LIST

		No. Copies
1.	Defense Documentation Center Cameron Station Alexandria, Virginia 22314	2
2.	Library, Code 0212 Naval Postgraduate School Monterey, California 93940	2
3.	Professor D. H. Nguyen Department of Mechanical Engineering Naval Postgraduate School Monterey, California 93940	1
4.	Commander M. T. Slayton Pearl Harbor Naval Shipyard Box 400 F.P.O. San Francisco, California 96610	1

DOCUMENT CONTROL DATA - R & D

(Security classification of title, body of abstract and indexing annotation must be entered when the overall report is classified)

1. ORIGINATING ACTIVITY (Corporate author)
Naval Postgraduate School
Monterey, California 93940

2a. REPORT SECURITY CLASSIFICATION
Unclassified

2b. GROUP

3. REPORT TITLE
AGE AND THERMAL DIFFUSION LENGTH OF PLUTONIUM-BERYLLIUM NEUTRONS IN POISONED WATER

4. DESCRIPTIVE NOTES (Type of report and inclusive dates)
Master's Thesis; June 1970

5. AUTHOR(S) (First name, middle initial, last name)
Marshall Thomas Slayton, Commander, United States Navy

6. REPORT DATE
June 1970

7a. TOTAL NO. OF PAGES
92

7b. NO. OF REFS
19

8a. CONTRACT OR GRANT NO.

b. PROJECT NO.

c.

d.

9a. ORIGINATOR'S REPORT NUMBER(S)

9b. OTHER REPORT NO(S) (Any other numbers that may be assigned this report)

10. DISTRIBUTION STATEMENT
This document has been approved for public release and sale; its distribution is unlimited.

11. SUPPLEMENTARY NOTES

12. SPONSORING MILITARY ACTIVITY
Naval Postgraduate School
Monterey, California 93940

13. ABSTRACT

Measurements of Pu-Be neutron age to indium resonance and thermal migration area were made in pure water at 24°C and in mixtures containing 1.16, 8.96, 27.81, 46.65, 70.09, and 80.09 grams/liter of boric acid at 40°C. Thermal diffusion lengths were calculated from these measurements and the dependence on poison concentration observed. It was concluded, both from failure of the age measurement and the irresolute thermal flux behavior at the heaviest poison concentration, that the "maximum absorption" limit was exceeded in this experiment. The absorption cross-section of the supporting medium corresponding to the 80.09 g/l concentration was 0.6120 cm^{-1}. The present results, together with previous experimental data, provide an estimate of diffusion length at the absorption limit of 0.5 cm, slightly less than that corresponding to the theoretical Corngold limit (0.6 cm).

KEY WORDS	LINK A		LINK B		LINK C	
	ROLE	WT	ROLE	WT	ROLE	WT
DIFFUSION LENGTH						
NEUTRON AGE						
PLUTONIUM-BERYLLIUM						
MIGRATION AREA						
BORIC ACID						
ABSORPTION						
THERMAL FLUX						

Thesis
S5703
c.1

120096

Slayton
Age and thermal diffusion length of plutonium-beryllium neutrons in poisoned water.